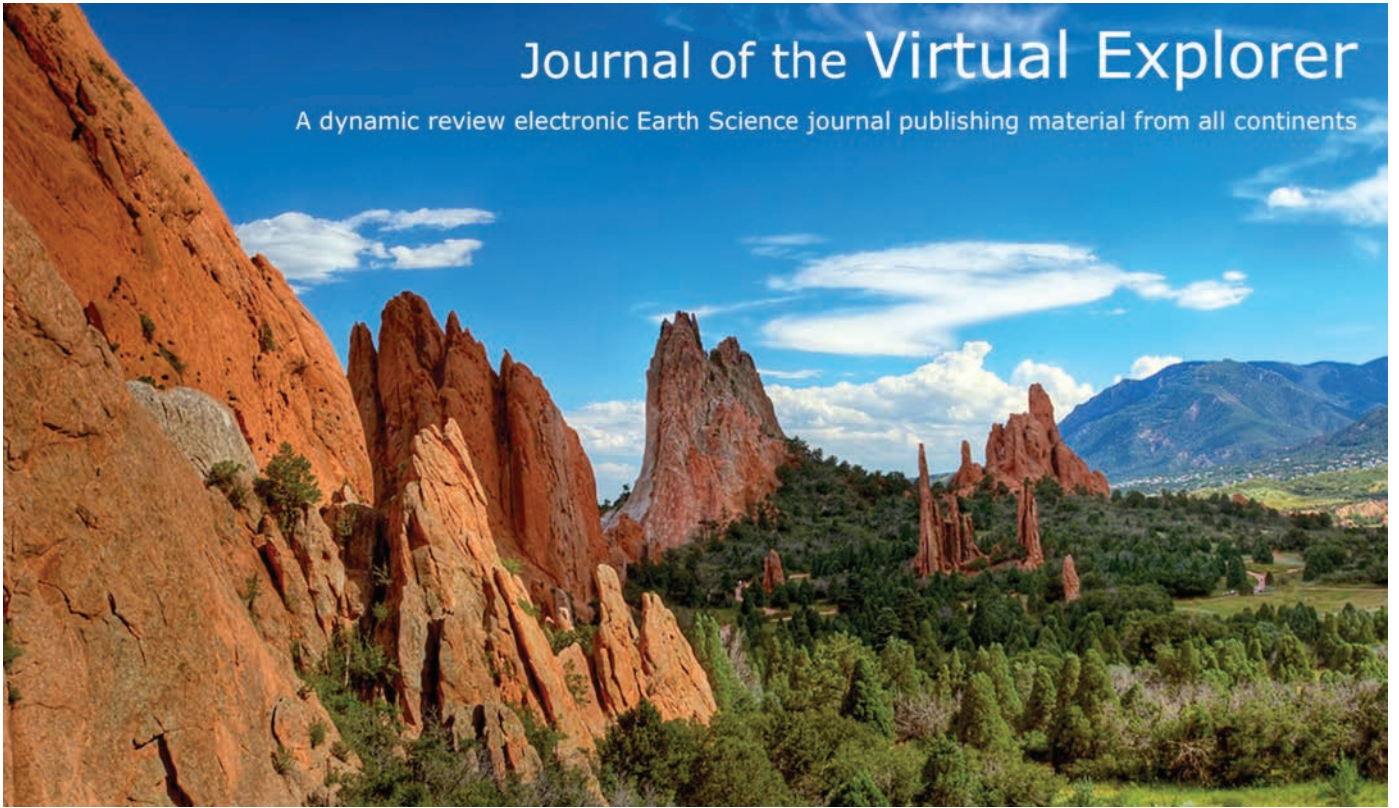


# Journal of the Virtual Explorer

A dynamic review electronic Earth Science journal publishing material from all continents



---

## **A geological journey through the deepest gorge on Earth: the Kali Gandaki valley section, west-central Nepal**

*Carosi R., Gemignani L., Godin L., Iaccarino S., Larson K. P., Montomoli C., Rai S. M.*

Journal of the VIRTUAL EXPLORER, Electronic Edition, ISSN 1441-8142, volume 47, Paper 7,  
In: (Eds) Chiara Montomoli, Rodolfo Carosi, Rick Law, Sandeep Singh, Santa Man Rai, Geolog-  
ical field trips in the Himalaya, Karakoram and Tibet, 2014

---

Download from: <http://virtualexplorer.com.au/papers/viewpdfink/337>

Click <http://virtualexplorer.com.au/subscribe/> to subscribe to the Virtual Explorer  
Email [team@virtualexplorer.com.au](mailto:team@virtualexplorer.com.au) to contact a member of the Virtual Explorer team

---

Copyright is shared by The Virtual Explorer Pty Ltd with authors of individual contributions. Individual authors may use a single figure and/or a table and/or a brief paragraph or two of text in a subsequent work, provided this work is of a scientific nature, and intended for use in a learned journal, book or other peer reviewed publication. Copies of this article may be made in unlimited numbers for use in a classroom, to further education and science. The Virtual Explorer Pty Ltd is a scientific publisher and intends that appropriate professional standards be met in any of its publications.

## A geological journey through the deepest gorge on Earth: the Kali Gandaki valley section, west-central Nepal

Carosi R. <sup>1</sup>, Gemignani L. <sup>2</sup>, Godin L. <sup>3</sup>, Iaccarino S. <sup>4</sup>, Larson K. P. <sup>5</sup>, Montomoli C. <sup>4</sup>, Rai S. M. <sup>6</sup>

<sup>1</sup>Department of Earth Sciences, University of Torino, via Valperga Caluso 35, I-10125, Torino, Italy.

<sup>2</sup>Department of Earth Science, Faculty of Earth and Life Sciences VU University, The Netherlands.

<sup>3</sup>Queen's University, Department of Geological Sciences and Geological Engineering, Kingston, Canada.

<sup>4</sup>Department of Earth Sciences, University of Pisa, via S. Maria 53, I-56126, Pisa, Italy

<sup>5</sup> Earth and Environmental Sciences, IKBSAS, University of British Columbia Okanagan, 3247 University Way, Kelowna, BC V1V 1V7, Canada.

<sup>6</sup> Department of Geology, Tribhuvan University, Ghantaghar, Kathmandu, Nepal.

### GUIDE INFO

#### Keywords

Lesser Himalaya  
South Tibetan Detachment  
Migmatites  
Greater Himalaya  
Tethyan Sedimentary  
Sequence

#### Citation

Carosi, R., Gemignani, L., Godin, L., Iaccarino, S., Larson, K., Montomoli, C. and Rai, S. 2014. A geological journey through the deepest gorge on Earth: the Kali Gandaki valley section, central Nepal. In: (Eds.) Chiara Montomoli, Rodolfo Carosi, Rick Law, Sandeep Singh, and Santa Man Rai, Geological field trips in the Himalaya, Karakoram and Tibet, Journal of the Virtual Explorer, Electronic Edition, ISSN 1441-8142, volume 47, paper 7, DOI: 10.3809/jvirtex.2014.00337.

**Correspondence to:**  
carosi@dst.unipi.it

### IN THIS GUIDE

The Kali Gandaki valley in the Central Himalaya is flanked by the eight thousand meter high Annapurna and Dhaulagiri massifs forming the deepest gorge in the world. It offers an invaluable opportunity to directly observe a cross section through the continental crust involved in the Himalayan orogen. The north-south trend of the valley runs almost perpendicular to the dominant regional strike and cross cuts the major tectonic units that comprise the Himalaya including the Lesser Himalayan Sequence, the Greater Himalayan Sequence and the Tethyan Sedimentary Sequence. The valley is easily accessible compared to many other sections across the belt and its history as a popular trekking route ensures services and lodging that are often not available elsewhere. We propose a one-week itinerary across the low metamorphic grade Proterozoic quartzites of the Lesser Himalayan Sequence in the south, through the high-grade, migmatitic metamorphic core of the Greater Himalayan Sequence to the unmetamorphosed Cretaceous age sedimentary rocks of the Tethyan Sedimentary Sequence to the north. This line of section allows observation of major, orogenic-scale tectonic faults/shear zones such as the Main Central Thrust and the South Tibetan Detachment, which bound the bottom and top of the high-grade core respectively, as well as other important shear zones within the Greater Himalayan Sequence (i.e. Kalopani shear zone). The Kali Gandaki section also offers spectacular examples of both mesoscopic and mountain-scale deformation structures including km-scale north-verging folds within the Tethyan Sedimentary Sequence.

### INTRODUCTION

The Kali Gandaki valley, located in the Mustang-Myagdi region of central Nepal, is a deep north-south trending feature that cuts across the main Himalayan belt. The Kali Gandaki river cuts a gorge > 6000 m in deep in between some of the highest peaks of the Himalayan range, west of Mt. Manaslu (Figs. 1, 2), including Dhaulagiri (8167 m) to the west and Nilgiri (7003 m) and Annapur-

na (8091 m) to the east.

The valley cross-cuts the major tectono-stratigraphic units of the Central Himalayan belt (Fig. 1) affording an excellent opportunity for their examination (e. g. Colchen et al. 1986; Vannay and Hodges, 1996; Godin, 2003; Upreti and Yoshida, 2005; Larson and Godin, 2009) (Figs. 1, 2). These units include: (1) the Tethyan Sedimentary Sequence (TSS), an almost continuous 10 km-thick

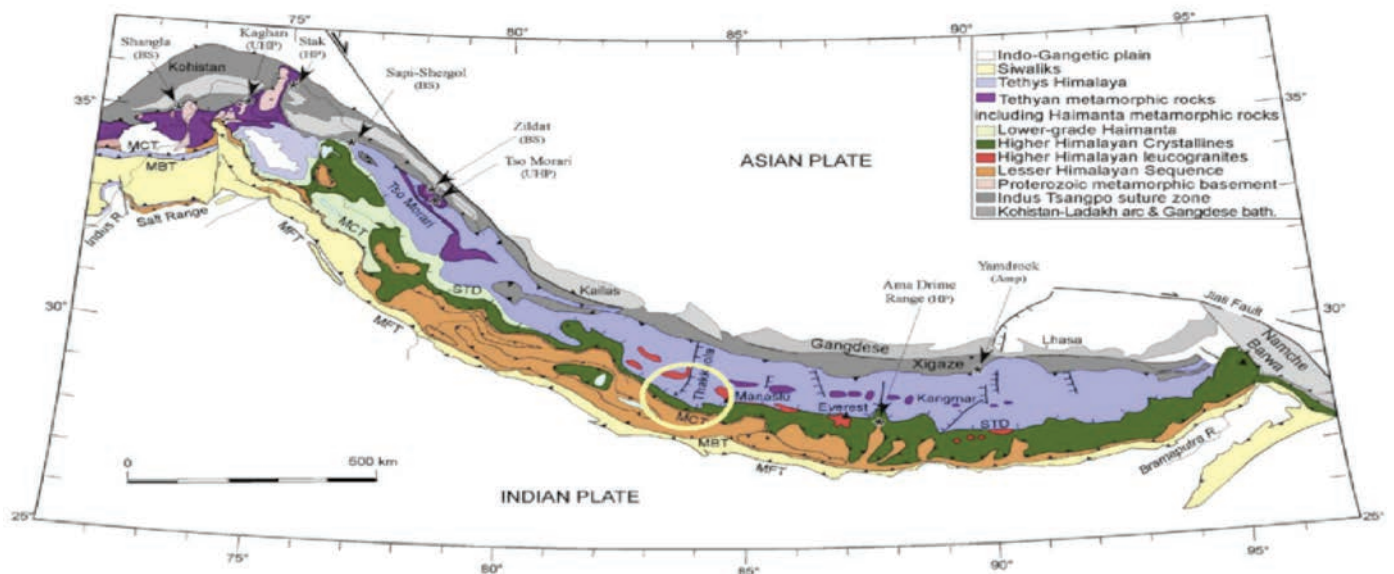


**Figure 1**  
Geological sketch map of the Himalayas showing the main tectonic units and location of the Kali Gandaki valley and Thakkola graben. From S. Guillot, website.



**Figure 2**  
North-South panoramic view of the main tectonic units in the Kali Gandaki valley from the Lesser Himalayan Sequence (South) to the Tethyan Sedimentary Sequence (North) through the Mt. Dhaulagiri and Mt. Tukuiche. View is from East to West.

early Paleozoic to early Tertiary in age sedimentary succession (Bordet et al., 1981; Colchen et al., 1986; Garzanti 1999; Godin et al., 1999a,b; Godin, 2003; Kellett and Godin, 2009; Myrow et al., 2009), (2) the Greater Himalayan Sequence (GHS), the metamorphic core of the Himalayan orogen, a 20-30 km thick sequence of medium to high-grade metamorphic rocks intruded locally by Miocene leucogranites (Vannay and Hodges, 1996; Visonà and Lombardo, 2002; Larson and Godin, 2009; Visonà et al., 2012), which is separated from the overlying Tethyan Sedimentary Sequence by the South Tibetan Detachment (STD) (Godin, 2003) or Annapurna Detachment in the Kali Gandaki valley and, (3) the Lesser Himalaya Sequence (LHS), which consists of Precambrian to Mesozoic un-metamorphosed to low-grade metamorphic sediments, which is over-thrust by the Greater Himalayan sequence across the Main Central Thrust (MCT) (Le Fort, 1975).

This field trip describes an itinerary running from the TSS, through the GHS and ending in the LHS. Some of the stops described here partly correspond to the stops reported in field guidebook by Upreti and Yoshida (2005), a recent and com-

prehensive field guide book that describes several aspects of the geology and natural hazards of the Kali Gandaki valley.

We approach to the geological stops (Fig. 3) in the same order as proposed by Upreti and Yoshida (2005). The starting point is the village of Jomsom (2720 m), which can be reached by either jeep or bus via the relatively new dirt road from Beni to Muktinath, or by a small aircraft from Pokhara airport. From Jomsom we suggest to first travel to the north to Muktinath (3700 m) through the Tethyan Sedimentary Sequence and then follow the valley back down to the south through the Greater Himalayan Sequence and finally Lesser Himalayan Sequence to Beni in the lowermost part of the valley (Fig. 3). From Beni it is possible to catch a bus to Pokhara and from here to reach Kathmandu by either land or air.

For background information relevant to the trip the main tectonic units are briefly described hereafter from the top to the bottom.

We describe the deformation structures in the units using the classical structural nomenclature indicating for example foliations as S1, S2 and so on. Each unit, however, records unique tectonic

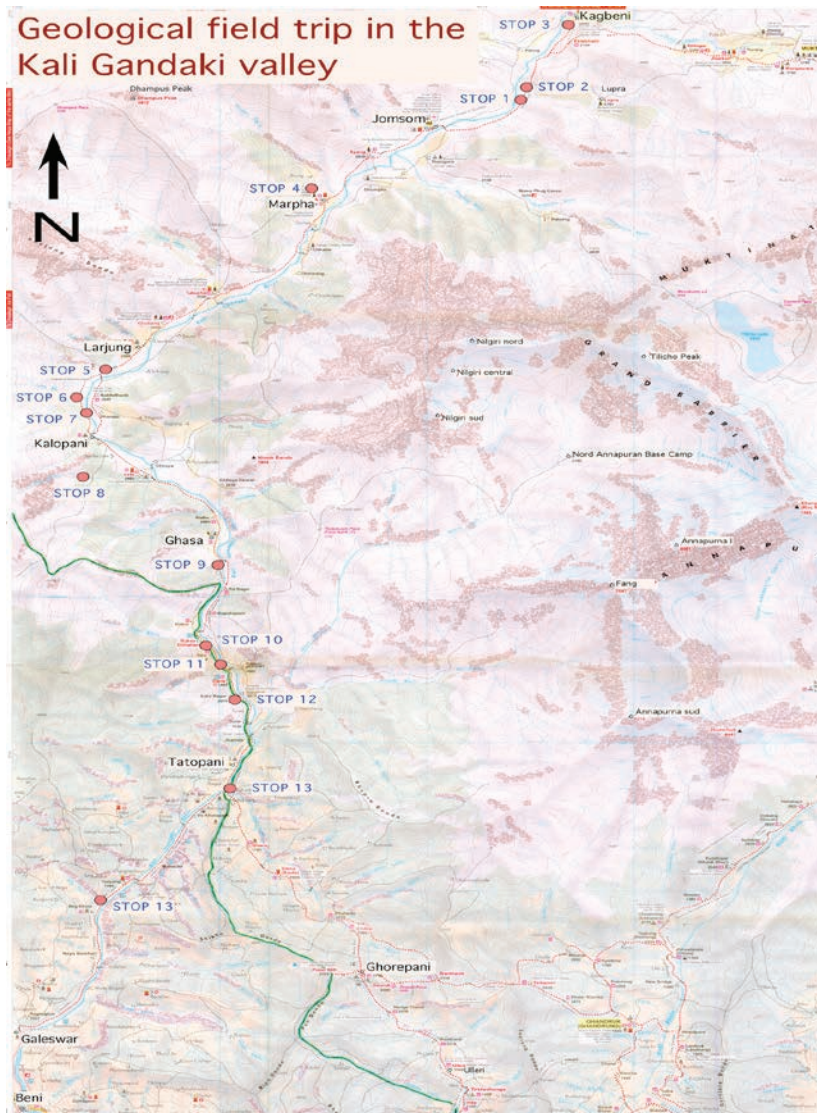


**Figure 3**  
Localization of the stops in the Kali Gandaki Valley (topographic base modified from NepaMaps).

and metamorphic histories and as such the foliations, folds and structural elements cannot be correlated across them even if they are indicated by the same letters and numbers; S1, L1 etc. for the TSS does not correspond to similarly labeled structures in the GHS or LHS.

### TETHYAN SEDIMENTARY SEQUENCE

In the central Nepal Himalaya, the TSS is a ~10 km thick unmetamorphosed to weakly metamorphosed Palaeozoic and Mesozoic sedimentary sequence, which was deposited on the northern Indian palaeocontinental margin and subsequently deformed during Himalayan orogenesis (Heim and Gansser, 1939; Gansser 1964; Fuchs, 1964;

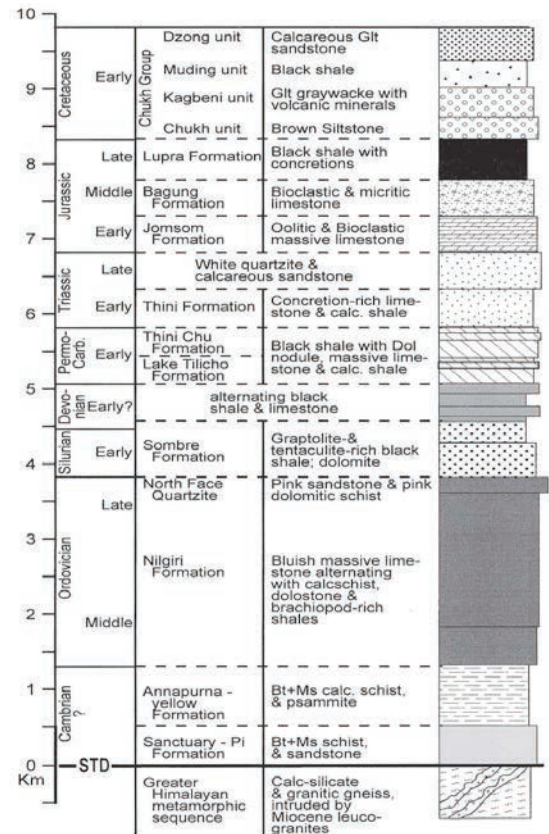


**Figure 4**  
Tethyan Sedimentary Sequence stratigraphic column (Godin, 2003; Searle & Godin, 2003).

Fuchs 1967; Bordet et al. 1981). The TSS is bound to the north by the Indus-Tsangpo suture zone (Fig. 1) and to the south by the STD, separating it from the lower Greater Himalayan Sequence (Yin, 2006; Antolin et al., 2011) (Figs. 1, 2). The TSS represents the evolution of the Paleo-Tethys Sea, from the pre-rift stage (Cambrian–Ordovician) to the final break-up of Gondwana in Early Cretaceous (Gaetani et al., 1991; see Garzanti, 1999 for a detailed stratigraphic framework; Fig. 4).

In the Kali Gandaki valley, the Paleozoic section is characterized by massive limestone, calcareous shale and pelite, with local dolomite and quartzite horizons. The lowest part of this section is the Sanctuary Formation (Fig. 5; Pêcher, 1978), which comprises highly deformed black schist, sandstone and limestone. In the Annapurna area, it has only been observed on the Thulo Bugin ridge, in the core of the refolded Fang nappe. Overlying the Sanctuary Formation is the Annapurna Formation (also known as the Yellow Formation or the Larjung series: Bordet et al., 1981; Colchen et al., 1981, Colchen et al., 1986;), which

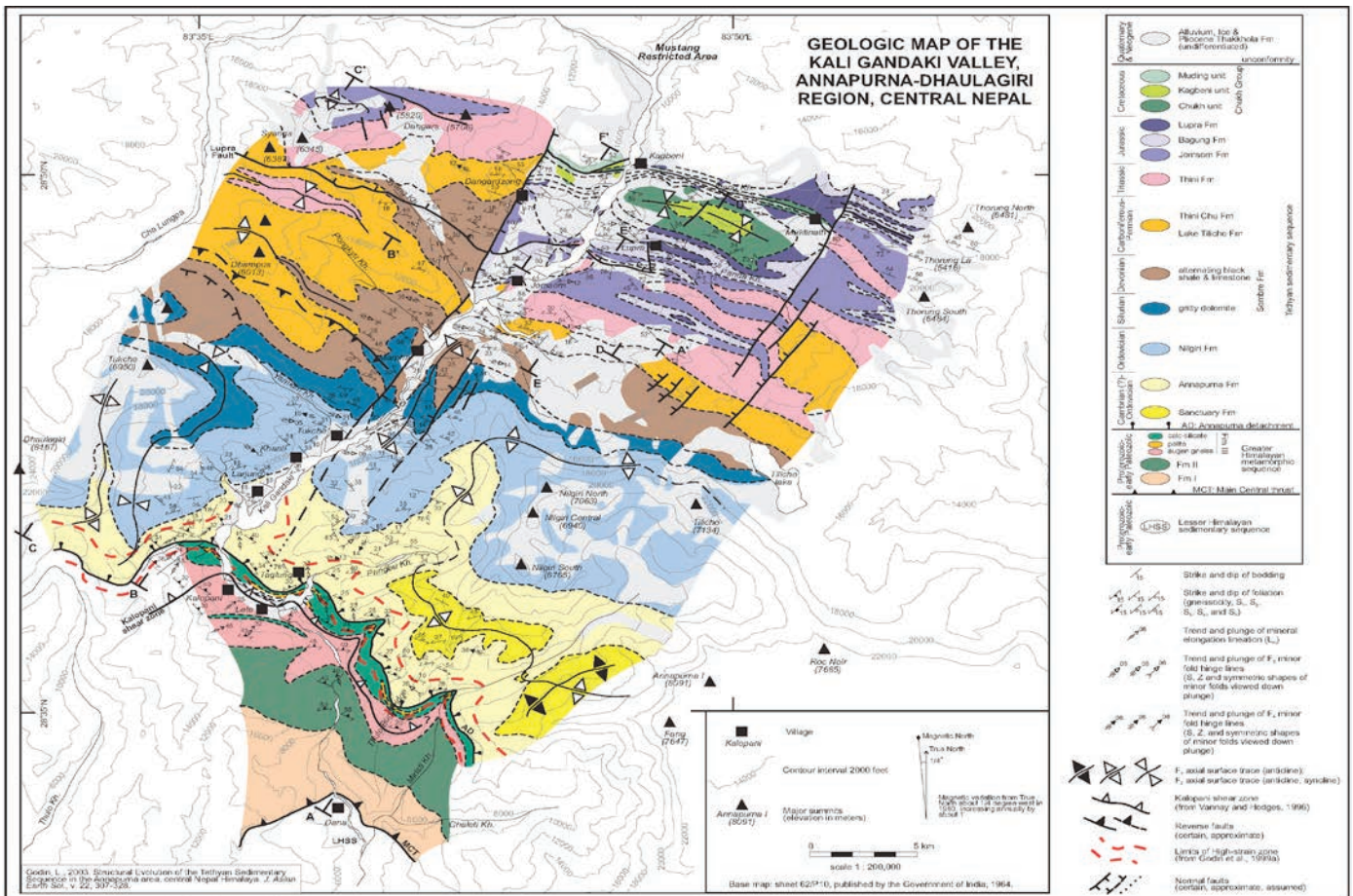


**Figure 5**  
Geological map of the upper Kali Gandaki valley (Godin, 2003).

is composed of calcareous biotite-grade psammitic and semi-pelitic schist and phyllite. Although they yield no direct chronologic constraints, the Sanctuary and Annapurna Formations have been interpreted as being Cambrian because they lie stratigraphically below the Ordovician Nilgiri Formation (Bordet et al., 1981). The overlying Nilgiri Formation comprises gray micritic limestone, grading upwards into pink dolomitic sandstone, calcareous shale, and siltstone. The Ordovician series is capped by a 400 m-thick calcareous arkose and siltstone unit termed the North Face quartzite (Bodenhausen et al., 1964). The upper portion of the Paleozoic is composed of alternating gritty dolomite, black shale, and limestone of the Sombre Formation (Silurian–Devonian), correlative with the Dark Band Formation of the Dolpo area, northwest of the Thakkhola region (Fig. 5; Fuchs, 1977). The Carboniferous–Permian units consist of a turbidite sequence dominated by calcareous shale with a minor siliciclastic contribution (Lake Tilicho and Thini Chu Formations; Bordet et al., 1981). The Mesozoic stratigraphy essentially comprises Triassic calcareous shale (Thini For-

mation), grading upwards to Jurassic fossiliferous limestone and black shale (Jomsom, Bagung and Lupra Formations), which are capped by the detrital units (conglomerates, sandstones) of the Lower Cretaceous Chukh Group (Bordet et al., 1981; Gradstein et al., 1992).

In the upper Kali Gandaki valley (Figs 5, 6), the Tethyan Sedimentary Sequence has undergone a complex structural evolution characterized by five deformational events (Godin, 2003; Kellett and Godin, 2009): southwest-verging isoclinal folds (D1); northeast-verging, tight, megascopic folds (D2); ductile extensional transposition at the base of the Tethyan sedimentary sequence along the north-dipping Annapurna detachment (D3) and related high-strain zone (Dt of Godin et al. 1999a); post-peak metamorphic, southwest-verging kink folds (D4) with related crenulation cleavages; and lastly northeast-trending, steeply dipping normal faults and spaced cleavages (D5) related to the Thakkhola graben system (Fort et al., 1982; Hurtado et al., 2001). The Tethyan Sedimentary Sequence has experienced only very low-grade to low-grade (<350°C) metamorphic conditions

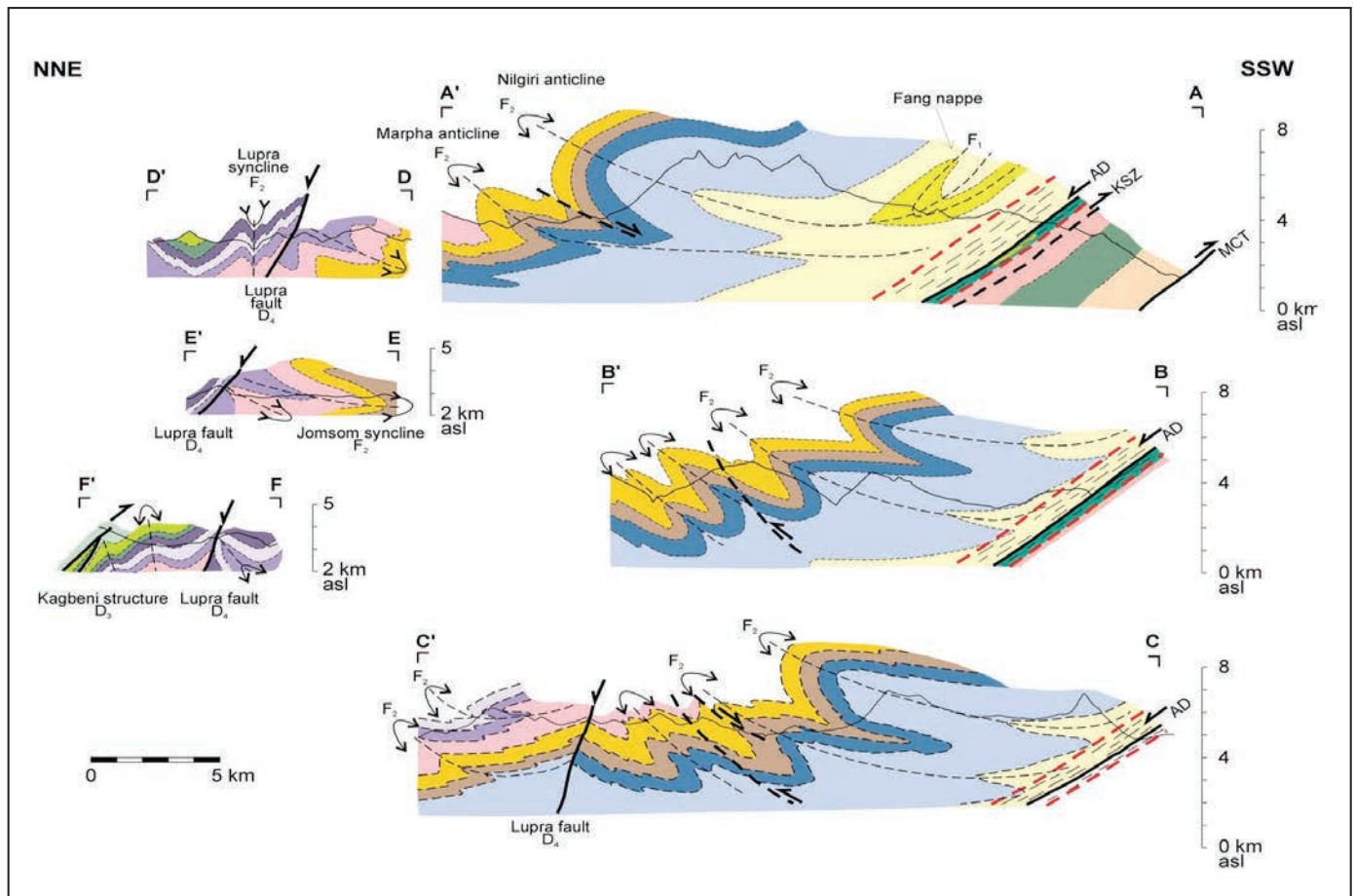


**Figure 6**  
Structural cross-sections of the Tethyan Sedimentary Sequence (Godin, 2003).

with temperature increasing to the base of the TSS (Fuchs and Frank, 1970; Colchen et al., 1986; Garzanti et al., 1994; Carosi et al., 2007; Crouzet et al., 2007; Dunkl et al., 2011).

The second deformation phase (D2) dominates the structural character of the Tethyan Sedimentary Sequence with prominent north-verging structures (Godin et al. 1999a; Godin 2003; Kellett and Godin, 2009; Figs. 7, 8). The absolute age of the D2 folds is uncertain, although cross-cutting relationships indicate that they predate the dominant Miocene motion along the STDS at ~21 Ma (Guillot et al., 1993; Godin et al., 1999a; 2001; Kellett and Godin, 2009). Searle (2010) consider F2 folds contemporaneous to the motion of the STDS. Palinspastic bed length restoration of the north-verging folds implies a minimum 35% shortening, and a minimum 150% vertical thickening (Fig. 6; Godin, 2003; Kellett and Godin, 2009). These data indicate that north-verging folds played a significant role in pre-Miocene crustal thickening (150-180% thickening of 12 km stratigraphy = approximately 20 km-thick) of the Himalaya, possibly predating or coinciding with Eocene-Oligocene burial metamorphism (ca. 43-35 Ma) preserved in the un-

derlying Greater Himalayan sequence (Godin et al., 1999a, 2001; Aikman et al., 2008; Carosi et al., 2010, in press).

Competing models have been proposed to explain the presence of hinterland-verging folds (F2) in the Tethyan sedimentary sequence of central Nepal. Early works suggested that these folds were formed by gravity-induced sliding and drag folding coeval with motion along the STDS (Bordet et al. 1981; Colchen et al., 1981; Burg and Chen 1984; Burchfiel and Royden, 1985; Burchfiel et al. 1992; Searle, 2010). Others proposed that the north-verging folds represent features related to an early compression and crustal-thickening event that occurred prior to Miocene displacement along the STDS (Godin et al., 1999a, 2001). Alternatively, it has been suggested that the north-verging folds may have developed while the STDS was the active upper boundary of southward-extruding Greater Himalayan sequence rocks; the folds recording the opposite shear drag folding effect of a flowing mid-crustal channel (Carosi et al., 2007). More recently, Kellett and Godin (2009) argued that drag TSS associated with the southward transport of the mid-crustal

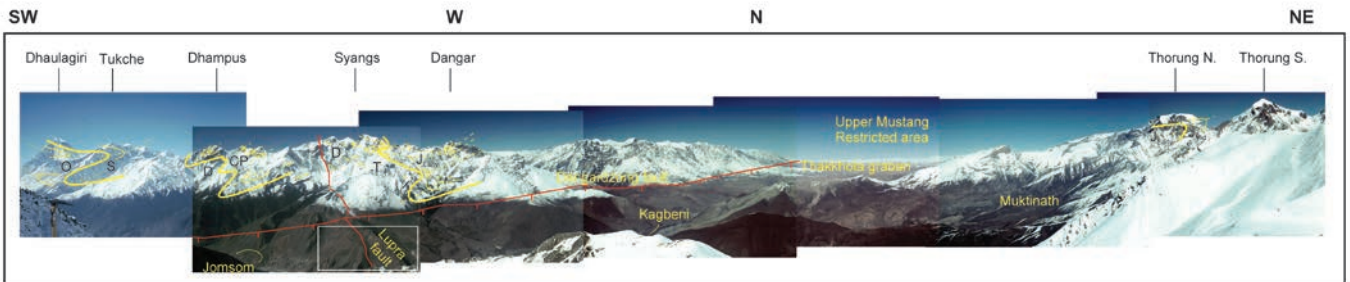


Figure 7  
Panorama of west ridge of Kali from Dhaulagiri to Dangar summits (Godin, 1999; 2003).

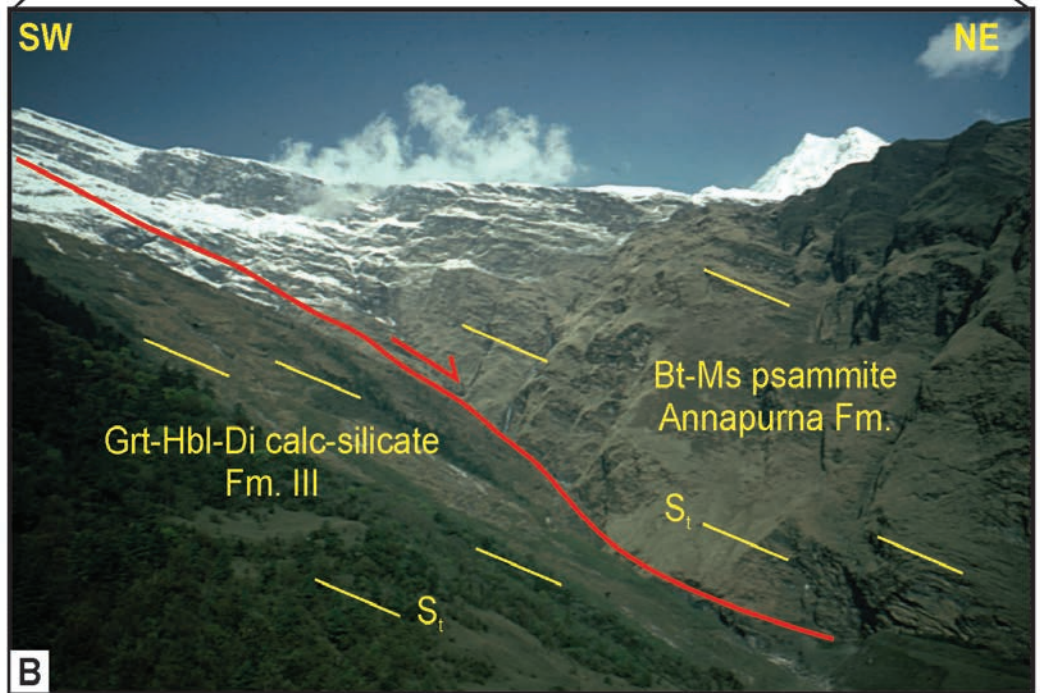
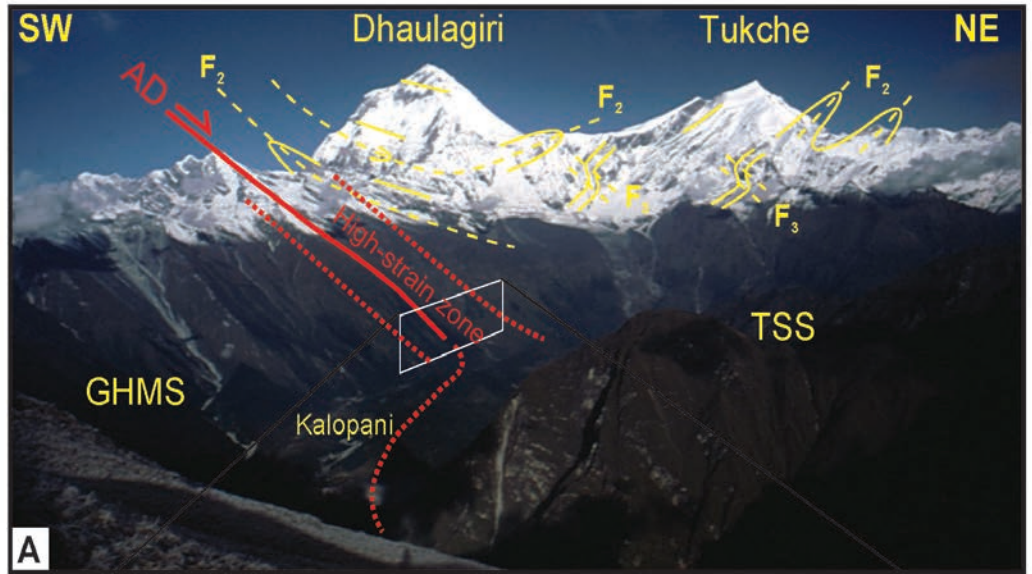


Figure 8  
Panorama from Thulo Bugin and zoomed-in cliff.

Greater Himalayan sequence may have modified the geometry of already existing folds, causing the northward vergence of the folds in the TSS. This latter model has recently been kinematically validated through centrifuge analogue modeling (Godin et al., 2011).

The north-dipping, extensional Annapurna detachment, a segment of the South Tibetan detachment system, separates the base of the Tethyan sedimentary sequence from the GHS (Brown and Nazarchuk, 1993). Mapping and structural analysis reveals the presence of a 1500 m-thick high-strain zone localized in the lowermost part of the Tethyan sedimentary sequence (in the Larjung Formation) and the uppermost part of the GHS, which is linked kinematically with normal-sense ductile shearing associated with the Annapurna detachment (Godin et al., 1999a). Near Larjung, 1500 m structurally above the base of the TSS, the primary stratigraphy and D1 and D2 structures are transposed into parallelism with this broad high-strain zone, and only one penetrative fabric (S3) with an associated down-dip mineral lineation (Lm) is generally preserved (Godin, 2003). Local crosscutting relationships are observed between S2 and S3, implying that the F2 northeast-verging folds predate the penetrative fabric associated with the high-strain zone (Godin, 2003). Within the Annapurna detachment zone, shear-sense indicators consistently indicate down-to-the-northeast normal shearing (see detailed analysis in Godin et al. 1999a). However, several lines of evidence, such as asymmetric kink folds affecting partly annealed quartz ribbons (Fig. 8a of Godin et al. 1999a), also indicate that the high-strain zone was affected by subsequent localized southwest-verging deformation attributed to the D4 event.

## GREATER HIMALAYAN SEQUENCE

The metamorphic core of the Himalaya is represented by the GHS, a continuous belt of high-grade metasedimentary and meta-igneous rocks with associated Miocene leucogranites (Carosi et al., 1999; Visonà & Lombardo 2002; Upreti, 1999; Hodges 2000; Visonà et al., 2012). This litho-tectonic unit typically forms the central part of the belt and is often associated with the highest topographic relief. The GHS occurs in the footwall of the STDS and is itself over-thrust atop the LHS

along the Main Central thrust (MCT). The MCT is a controversial tectonic feature and has variably been described as a wide zone (up to 4-5 km some sections) of deformation is characterized by mylonites locally overprinted by cataclasites (Carosi et al., 2002, 2007), a structure associated with the kyanite isograd (e.g. Le Fort, 1975) and an inverted field metamorphic gradient, a break in Nd isotopes (e.g. Robinson et al., 2001), a break in U-Pb detrital zircon ages (e.g. Parrish and Hodges 1996), or a strain gradient at the base of rocks metamorphosed and cooled during the Miocene evolution of the mountain belt (Searle et al., 2008). The main foliation strikes NW-SE, dips moderately to the NE with down-dip object lineations and typically records a top-to-the SW sense of shear (Colchen et al., 1986; Hodges, 2000). In this guide we put the MCT just above Dana village, accordingly to the original definition of Le Fort (1975) and Colchen (1986) which separates the kyanite and garnet bearing gneiss of the GHS from the lower quartzites of the LHS.

Le Fort, (1975) recognized three formations, which were later re-considered as tectonic units (Searle and Godin, 2003).

- Unit 1. The base of the GHS consists of predominantly clastic metasedimentary rocks, represented by biotite-muscovite-garnet-kyanite gneisses, although mica schists and phyllites, calc-schists, quartzites, para-amphibolites, and subordinate impure marbles are also present. Layering in the unit dips moderately northward in most exposures (Vannay and Hodges, 1996; Hodges, 2000; Rai et al., 2005). Unit 1 has been traditionally considered as a uniform crustal section with a variable thickness from 1 km to more than 20 km along strike (Le Fort, 1975).
- Unit 2. Unit 1 is overlain by a 2-4 km thick sequence of amphibolites-facies, banded calc-silicate gneiss, paragneiss, marble and amphibolite. The boundary between units 1 and 2 is parallel to the compositional layers in both packages of rocks. The lack of recognized tectonic or metamorphic discontinuities at the transition between the two units and the absence of localized tectonic fabrics, has been originally interpreted by some authors (Colchen et al., 1986) as an evidence to consider the two units as an unique block. The transition between the two units is gradual and highlighted by changes in mineral composition.
- Unit 3. The unit 3 comprises nearly homogeneous Cambrian-Ordovician orthogneiss (Pognante et al., 1990; Godin et al., 2001) that is intruded

by a network of Miocene sills and leucogranitic dykes. The intrusions may be related to the 4-5 km thick Manaslu leucogranite present few 10s of kilometers to the east, one of the larger granitic body within the Himalaya (Searle, 2010). The orthogneiss is disrupted by the ductile Kalopani Shear Zone (KSZ) (Vannay and Hodges, 1996; Godin et al., 1999b; Godin et al., 2001; Godin et al., 2003; Searle, 2010) (Fig. 5), which is characterized by highly strained orthogneiss and migmatitic gneiss. Isotopic Rb-Sr data indicate that the unit 3 protolith is Cambrian-Ordovician (Pognante et al., 1990), this is in agreement with U-Pb zircon ages (Godin et al., 2001).

The uppermost part of unit 3 is marked by the Annapurna Detachment (Figs. 5, 8), a shear zone that juxtaposes the orthogneiss of Unit 3 with rocks of the Largjung Formation. The Largjung Formation is characterized by poly-deformed metapelites and marbles. Colchen et al. (1986) considered these rocks as part of the TSS. Other studies, however, have included the Larjung Formation as part of the Unit 3 of the GHS (Vannay and Hodges, 1996). A similar situation is described in the adjacent Modi Khola valley and in the Marsyangdi valley between Annapurna and Manaslu massifs farther to the east (Figs. 1, 3), where calc-silicate rocks are mapped structurally above and below the orthogneiss of Unit 3. More recently Unit 3 is considered constituted by orthogneiss, metapelites, marbles and calc-silicates (Vannay and Hodges 1996; Godin et al., 2001; Searle, 2010).

The main fabric in the GHS is a pervasive, transposition foliation formed during a second deformation phase (S2; Carosi et al., 1999, 2007, 2010, in press). It is often recognizable as a shear band cleavage as defined by Passchier and Trouw (2005). The S2 foliation typically strikes NW-SE and dips 30°–60° toward the NE. It is marked by the preferred orientation of metamorphic minerals and recrystallized quartz ribbons. Kyanite, staurolite, muscovite, and biotite are occasionally bent or kinked along shear bands. Top-to-the-SW sense of shear is marked by C-S fabric, shear bands, asymmetric tails around porphyroclasts, and rotated garnets within the mylonites in the lower portion of the GHS. The elongation lineation (L2) trends NE-SW and plunges NE moderately to steeply (20°, 60°). S1, formed during D1 deformation, is sometimes preserved as a relict in D2 fold hinges (F2) and S2 microlithons and as internal foliation in porphyroblasts (Carosi et al.,

2010). The GHS underwent at least two later folding phases, characterized by nearly orthogonal NW-SE and NE-SW trending fold axes, resulting in kilometer-scale open folds with steeply dipping axial planes. These folds, well-expressed in western Nepal, affect the tectonic boundaries (see geological cross sections in Upreti (1999) and Carosi et al. (2002, 2007) and have also been described eastward in the Mt. Everest-Mt. Makalu region, Sikkim and Bhutan (Lombardo et al., 1993; Carosi et al., 1999; Schelling, 1992).

## LESSER HIMALAYAN SEQUENCE

The LHS, which is also referred to as the Midlands Group in central Nepal (Upreti, 1996), includes dolomite, limestone, impure quartzite, marble, phyllite, schist, orthogneisses and metabasaltic rocks. These rocks have been affected by greenschist to lower amphibolite facies metamorphism (Upreti 1999; Hodges, 2000). The LHS can be subdivided in two units interpreted to be separated by an unconformity (Upreti, 1999 with references). The lower unit or the “Lower Lesser Himalaya”, comprises sedimentary-volcaniclastic rocks and orthogneisses ranging in age from Paleo-proterozoic to Meso-Proterozoic (Upreti, 1999 and references therein). The upper unit, the “Upper Lesser Himalaya”, dominantly comprises carbonaceous phyllite and marble, associated quartzites, and graphitic rich rocks with middle Proterozoic protoliths.

The distinction between rocks of the GHS and rocks of the LHS is largely associated with the mapped location of the MCT. In this field guide we map the MCT approximately at the northern end of village of Dana (Fig. 3) and thus the rocks that crop out to the south in the interpreted footwall comprise the LHS. The LHS in the Kali Gandaki valley comprises an almost complete section beginning with the early Proterozoic Kuncha Formation at the lowest levels exposed and extending up to the middle Proterozoic Robang Formation (Larson and Godin, 2009). The Kuncha Formation comprises the bulk of the Lower Lesser Himalaya in the field trip area; it is a >5 km thick package of phyllitic schist and meta-sandstone. Conspicuously absent in the lower section along Kali Gandaki valley is the Paleoproterozoic (DeCelles et al., 2000) Ulleri augen orthogneiss, a km-scale thick band of mylonitized potassium

feldspar augen-bearing unit. This orthogneiss is well exposed at Ulleri village, south-east (about 3 km) of Deurali-Ghorepani village (Pêcher and Le Fort, 1986). The Ulleri, which has been interpreted as a syndepositional intrusion (Pêcher and Le Fort, 1977), occurs in the Kuncha Formation in adjacent valleys to the east (Colchen et al., 1986) and its equivalents are mapped across much of the central Himalaya.

The base of the Upper Lesser Himalaya in the study area is marked by quartzite of the Fagfog Formation (also referred to locally as the Ghandrung quartzite). The tectono-stratigraphy above the Fagfog Formation comprises a succession of alternating carbonaceous phyllitic schist and marble or dolostone units. These include from lower to higher position: (1) the interbedded carbonate rocks and phyllitic carbonaceous schist of the Dandagaon and Nourpul Formations, which cannot be separated in the Kali Gandadki, (2) the metadolostone and marble of the Dhading Formation, (3) the phyllitic schist and carbonaceous schist of the Benighat Formation with intercalated Jhiku carbonate beds, and (4) the conspicuous marble of the Malekhu Formation which is overlain by non-calcareous phyllitic schist (Larson and Godin, 2009).

Yoshida et al. (2005) and Rai et al. (2005) observed a series of highly sheared rocks (e. g. phyllonite, mylonite-ultramylonite and mylonitic granite, garnet-bearing gneiss and schist (total thickness about 700 m) between Duwari Khola to the south and the MCT, north of Dana. Field observation shows a sudden change in both lithology and metamorphic grade of these rocks compared with the underlying uppermost LHS rocks. This unit is interpreted to represent a higher grade metamorphic equivalent of the Lower LHS (Kuncha Formation and Ulleri type augen gneiss exposed at Ulleri village, south of Deurali-Ghorepani village). Therefore, a thrust locally named as the Duwari Khola Thrust (DKT) is placed at the contact between the mylonitic rocks in the north and the black schist of the upper LHS in the south. This 700 m thick sheared zone is considered as the MCT zone.

## ITINERARY

We start the itinerary walking from Jomsom village (2720 m) and we follow the dirt road to the

North up to Kagbeni village (2810 m). From here we come back from the same road cross-cutting all the three main tectonic units (TSS, GHS and LHS) and the STD and MCT.

## TSS Stops

### Stop 1

**Locality:** West bank between Lupra khola and Jomsom (N 28°47'55.19" E 83°45'27.74")

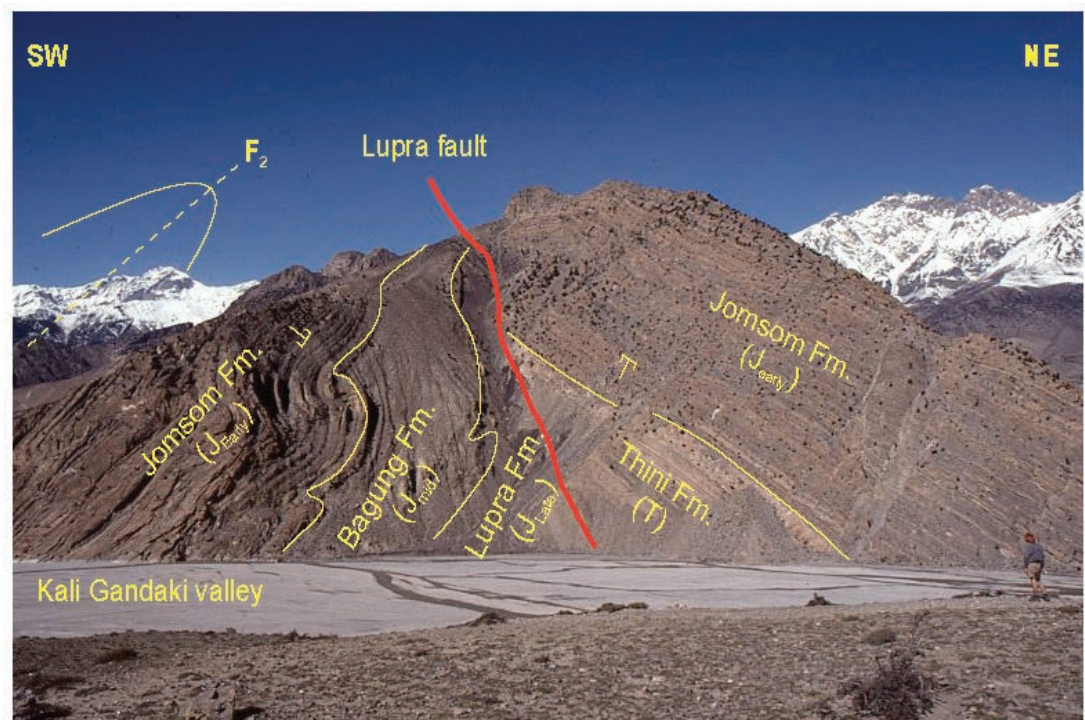
**Theme:** Lupra Fault. Large cliff, view from river bed (also good place to hunt for shelligrams in the river bed)

We move to the North and just after the old Jomsom village we can observe in the road cliff outcrops of the Jomsom Formation (Fig. 4) with alternating limestone, shale and sandstone. Crinoid ossicles, brachiopods and bivalves can be frequently observed.

The Lupra fault was first recognized by Colchen et al. (1986) and Gradstein et al. (1992), and subsequently studied in detail by Godin (2003). The Lupra fault is a steeply north-dipping, west-striking fault clearly visible in the cliffs above the Kali Gandaki river, a few kilometers north of Jomsom. The trace of the fault can be observed on the south slope of the Syang peaks where it marks a sharp structural break, and extends 20 km to the east. It terminates abruptly just south of the village of Lupra, where it is cut by a north-striking subsidiary fault of the Thakkhola graben system. It has not been observed east of this point. The Lupra fault is best expressed within the down-dropped block of the Thakkhola graben, where it has a greater offset. On the west bank of the Kali Gandaki river, the fault marks a sharp contrast between recumbent north-verging folds to the south, with a weakly folded homoclinal panel to the north. At this locality (Fig. 9), the footwall is composed of an overturned limb of a north-verging fold, within Jurassic rocks of the Jomsom, Bagung and Lupra Formations. The hanging wall consists of a north-dipping homoclinal panel of upright Triassic to Early Jurassic rocks (Thini and Jomsom Formations). Based on the stratigraphic evidence of this locality, the Lupra fault can be interpreted as a reverse fault that juxtaposes Triassic rocks in its hanging wall with Late Jurassic rocks in its footwall.

On the east bank of the Kali Gandaki, however, just south of the village of Lupra, the Lupra fault juxtaposes rocks of similar age (Lower Jurassic),

Figure 9  
Lupra fault from Kali  
Gandaki.



but with contrasting structural style. In this area, the Lupra fault marks the boundary between upright folds (higher structural level) in the hanging wall and recumbent folds (lower structural level) in the footwall. It therefore appears that the Lupra fault also marks a structural break in the north-verging fold belt. On this basis, the Lupra fault can be interpreted as a normal fault. Unfortunately, the fault trace is located under steep slopes mainly comprised of very friable shales of the Lupra Formation or on inaccessible cliff faces. Therefore, no fault-slip data, such as slickenlines, extensional fractures or stylolites have been observed. Significant strike-slip motion along the Lupra fault cannot be ruled out, although no such evidence has been found.

The only remnants of Cretaceous rocks of central Nepal are preserved within the Thakkhola graben (Bordet et al., 1981; Colchen et al., 1981). They are bounded by the Dangardzong fault to the west, the Muktinath fault to the east, and the Lupra fault to the south. Furthermore, the Lupra fault also marks the southern limit of the Pleistocene–Holocene lacustrine sediments that fill part of the Thakkhola graben, mainly comprising the flat plains of the Dangardzong and Phalla villages (Fort et al., 1982). The strong morphological expression of the Lupra fault within the Thakkhola graben, the higher-level structures and young sediments preserved in its hanging wall, and its

steeply dipping nature all support an important normal-sense component for the fault, and a possible link with the Thakkhola graben (Godin, 2003). The apparent old-over-young stratigraphic relationship visible in the Kali Gandaki could represent some earlier thrust motion along the fault plane (Godin, 2003).

#### Stop 2

**Locality:** Lupra village in the Lupra khola (optional side trip) (N 28°48'6.90" E 83°47'26.95")

**Theme:** Black shales of the Jurassic Lupra Formation, containing large ammonite and belemnite concretions. Lupra village – in the Lupra khola (optional side trip).

The 250 m thick Lupra Formation occurs over a distance of > 1500 km. It is likely more than double that thickness but intense, intra-formational deformation and pinching out renders accurate thickness estimation impossible in outcrop (Gradstein et al., 1992). The formation comprises paleo-to medium-grey to black shale, which increases in silt content upwards (Gradstein et al., 1992). Some organic-rich layers are present but lamination on a fine-scale appears to be absent (Gradstein et al., 1992).

The Lupra Formation is well known for its deep shelf to upper slope macrofossils (shallow-

Figure 10  
Lupra Shales above Lupra  
village.



Figure 11  
Lupra ammonite.



er paleoenvironments would not have sustained the variety of organisms) (Gradstein et al., 1992). The presence of abundant terrestrial, organic-rich laminae within the shale could indicate that there was land nearby, but it is much more likely that the material was transported long distances out onto the shelf-slope break position (Gradstein et al., 1992). Further evidence for a deep marine depositional environment is the lack of coarse clastic material or shallow-marine facies found in a coeval lateral position (Gradstein et al., 1992).

Concretions up to 1 m in diameter are common and typically have macrofossils – ammonites, belemnites, gastropods, brachiopods and bivalves – in their cores (Gradstein et al., 1992). The concretions are generally larger in the older strata with a higher proportion of smaller concretions at higher levels (Gradstein et al., 1992). Ammonites occur throughout and are locally abundant, especially in the younger portions of the formation (Gradstein et al., 1992). The concretions probably formed during shallow to deep burial; the preservation of

three-dimensional burrows in some concretions indicates that their initial growth preceded compaction (Gradstein et al., 1992). The Lupra shale is high in organic content, which was highly sought after by sulfate reducing bacteria. This reduction of the organic material formed pyrite, which often replaces the macrofossils' structures.

The unit is best exposed around the village of Lupra (Fig. 10; in the Lupra khola, east of the Kali Gandaki). However, concretions (Fig. 11) can be found amongst the cobbles and pebbles of the Kali Gandaki between Lupra Khola and Jomson.

### Stop 3

Locality: Kagbeni; (N 28°50'12.11" E 83°46'51.32")  
Theme: Kagbeni structure (reverse fault) in Early Cretaceous rocks with continental fossils (leaves, etc). Kagbeni – west bank across river (bridge). Careful not to cross northward into Mustang restricted area.

The sedimentary succession preserved in the Late Jurassic to Early Cretaceous strata of the Thakkhola region represents the passive-margin deposits accumulated during the break-up of Eastern Gondwana (Garzanti, 1999). Using paleomagnetic data it has been postulated that during the Early Cretaceous (and possibly as early as the Late Jurassic) Nepal was at a paleolatitude of approximately 38°S. At this latitude, conditions would have favored siliciclastic deposition—assuming that Mesozoic latitudinal distribution of sediment types is similar to the present day deposition—replacing the tropical carbonate paleoenvironments



**Figure 12**  
Panorama (3 photos) of Kagbeni structure; view from east.



**Figure 13**  
Fossil leaves in deltaic Chukh Group.

of the middle Jurassic (Gradstein et al., 1992).

Interestingly, the Early Cretaceous Chukh Group deltaic strata preserved in the Thakkhola region are coeval with regressive units found in northern Europe (“Wealden”) and North America (Gradstein et al., 1992). These rock units suggest the periodic uplift of the continental margin, and may possibly be associated with major first and second order eustatic sea level drops (Gradstein et al., 1992). The Chukh Group (Chukh, Kagbeni, and Muding units) contains rift-related volcaniclastic material that was derived from the coeval Taltung Formation of the Lesser Himalaya and transported northward to the Thakkhola region (Gradstein et al., 1992). Volcanic activity during the Early Cretaceous took place after the onset of sea-floor spreading and during the break-up between India and Australia (Gradstein et al., 1992). The Early Cretaceous ended with an overall drowning of the clastic depositional shelves (Garzanti, 1999).

The Chukh Group crops out in the tectonically folded and faulted anticline on the west bank of

the Kali Gandaki across from the village of Kagbeni (Fig. 12; Gradstein et al., 1992; Godin, 2003). The Kagbeni unit is found at the base and top of the Chukh unit at this locality due to structural duplication (Godin, 2003). It contains pebbles, large wood fragments and fossil leaves (Fig. 13; Gibling et al., 1994). The Chukh Group is interpreted to represent a delta complex in which the distributary channels and delta front environments are dominant (Gradstein et al., 1992; Gibling et al., 1994).

From here we move back to the south following the same road down to the beautiful Marpha village.

#### Stop 4

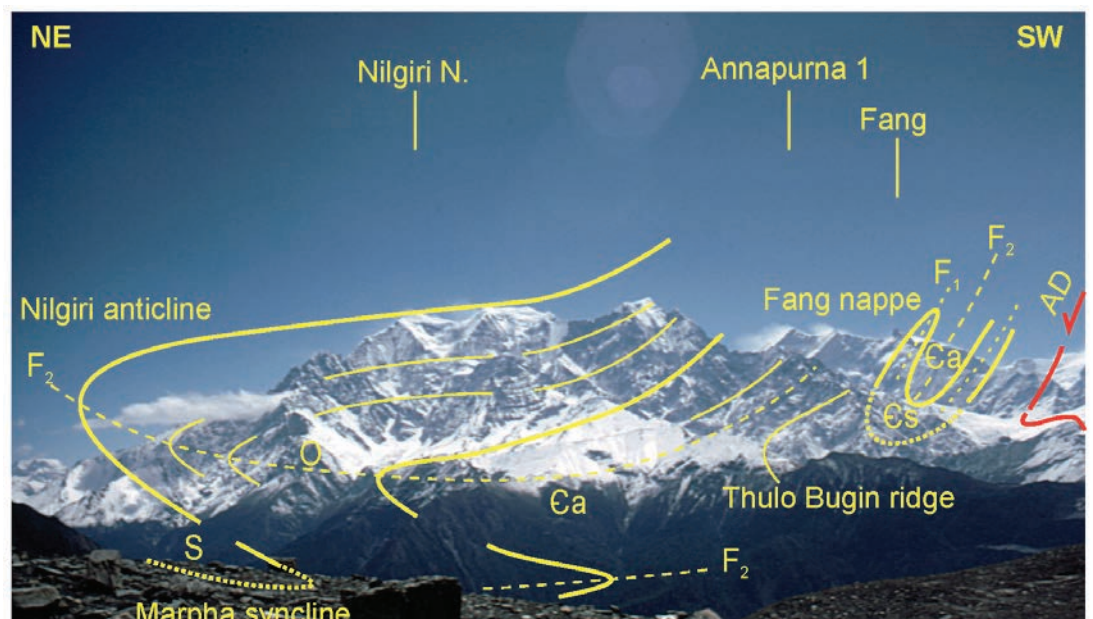
**Locality:** Marpha (along trail above Marpha Gompa – west bank of Kali; N 28°45’16.96” E 83°40’42.77”)

**Theme:** view across valley to west face of Nilgiri (North verging folds in the Ordovician limestone); also outcrop of fold interference pattern

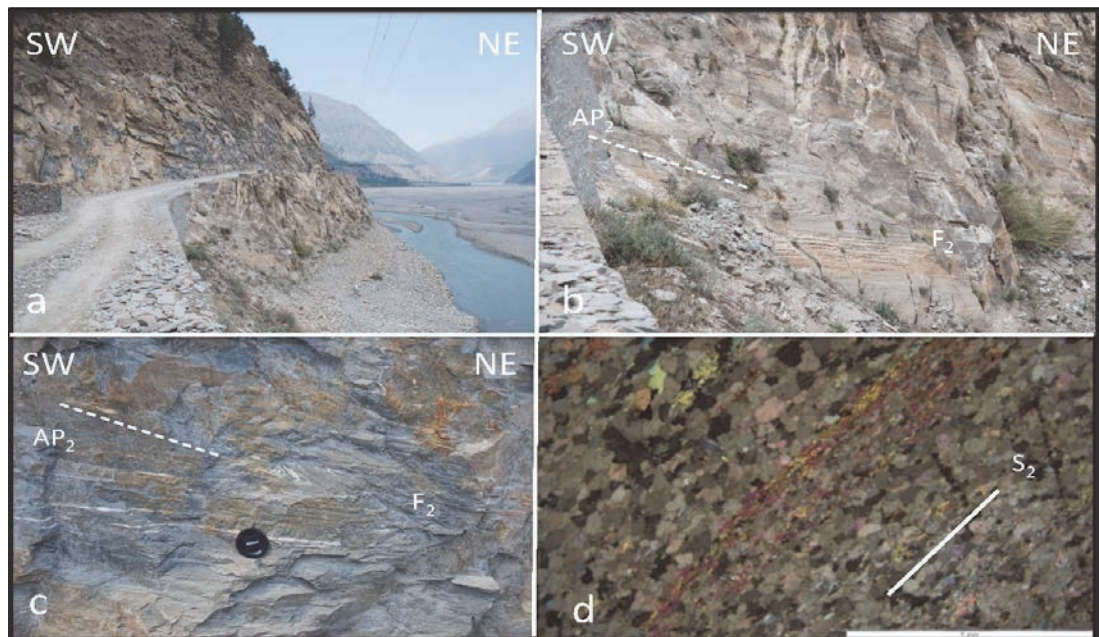
Figure 14  
Interference between F2-F3 folds in Sombre Formation.



Figure 15  
View east to Nilgiri anticline.



**Figure 16**  
Road cliff just south of Larjung village; (a) banded marbles of the Annapurna Yellow Formation; (b) F2 metric folds in the marble just below the road cut in a) folding the S1 foliation, (c) asymmetric F2 fold in the marble with gently dipping to the North D2 axial planes; (d) thin section of the marbles showing a SPO of calcite crystals along the S2 foliation.



#### F2-F3 in Silurian calcareous shales (Sombre Fm).

Hike up for approx. 1hr. (to elevation ~3,200m). The trail starts in the center of Marpha, just south of the Gompa (Buddhist temple) in the center of village. The trail shows exposure of Siluro-Devonian calcareous shales, displaying F2-F3 interference patterns (Fig. 14). This is also an excellent place to view the spectacular “Nilgiri” anticline: The F2 folds visible in the Kali Gandaki valley generally constitute structures parasitic to crustal-scale northeast verging folds visible on the west face of the Nilgiri Mountains, where Ordovician limestones are folded in a kilometer-scale overturned antiform (Fig. 15; Bordet et al., 1981). Macroscale examples of parasitic folds of the Nilgiri anticline include the Marpha anticline (visible on the east bank of the Kali Gandaki at Marpha) and the Jomsom syncline exposed on the east bank of the Kali Gandaki immediately north of Jomsom (Godin, 2003). These structures are part of a major fold train that extends at least to the upper reaches of the Kali Gandaki in the upper Mustang–Lo Manthang area 50 km north of Kagbeni.

#### Stop 5

Locality: south of Larjung village (N 20° 40' 57.33" E 83° 36' 41.70").

Theme: deformation in the marbles of the Annapurna Yellow Formation (Larjung Formation).

After the village of Larjung the cliff road cut exposes the banded marbles of the Annapurna Yellow

Formation with a penetrative foliation (in detail it is an S3 foliation according to Godin, 2003) that dips gently to the northeast (Fig. 16a). Metre to centimetre scale F2 folds can be observed folding the previous S0-1 foliation (Fig. 16b, c). The S2 foliation is marked by the shape preferred orientation of recrystallized calcite crystals as well as layers of white mica and biotite. (Fig. 16d). Stable isotope data from calcite and quartz indicates there is sharp decrease in temperature from nearly 580°C at the base of the Annapurna Yellow Formation to nearly 325°C in the higher part of the Nilgiri Formation (Montomoli et al., 2013). This temperature gradient is also reflected by changes in calcite deformation mechanisms and a decreasing upward grain size.

#### Stop 6

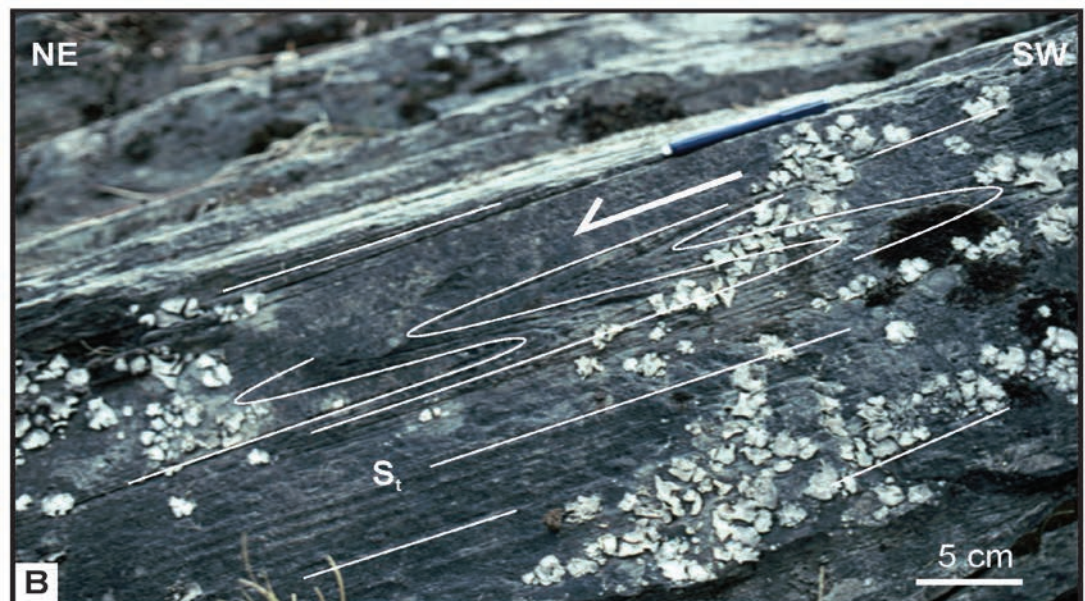
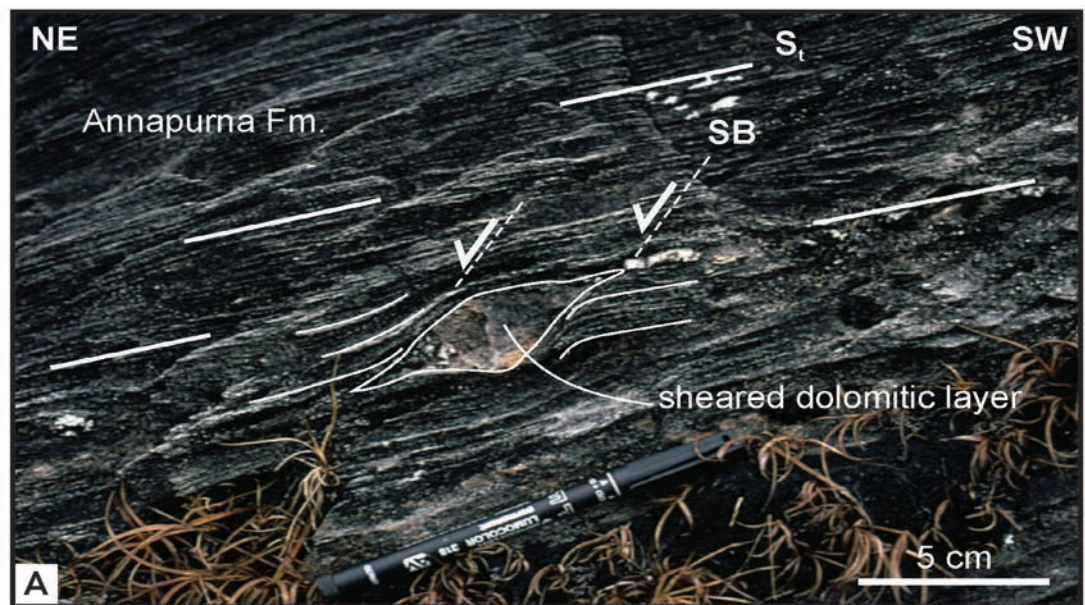
Locality: North of Kalopani; side khola at Kokhetanti (N 28°39'52.97"E 83°35'26.02").

Theme: STDS – with sheared Annapurna-Larjung-Yellow Fm, cross cut by 22 Ma leucogranitic dykes. Top north normal overprinted by reverse sense shear.

The contact between the Tethyan Sedimentary Sequence and the Greater Himalayan Sequence is visible in a stream gully at Kokhetanti, just northwest of the village of Kalopani; this corresponds to the Annapurna detachment, a segment of the South Tibetan detachment system (Figs. 1, 2). Gansser (1964) noted that although this contact appears conformable, it delineates a clear bounda-

Figure 17

Outcrop photos with shear sense indicators in the Annapurna Fm. A: sheared dolomitic layer; B: asymmetric folds.



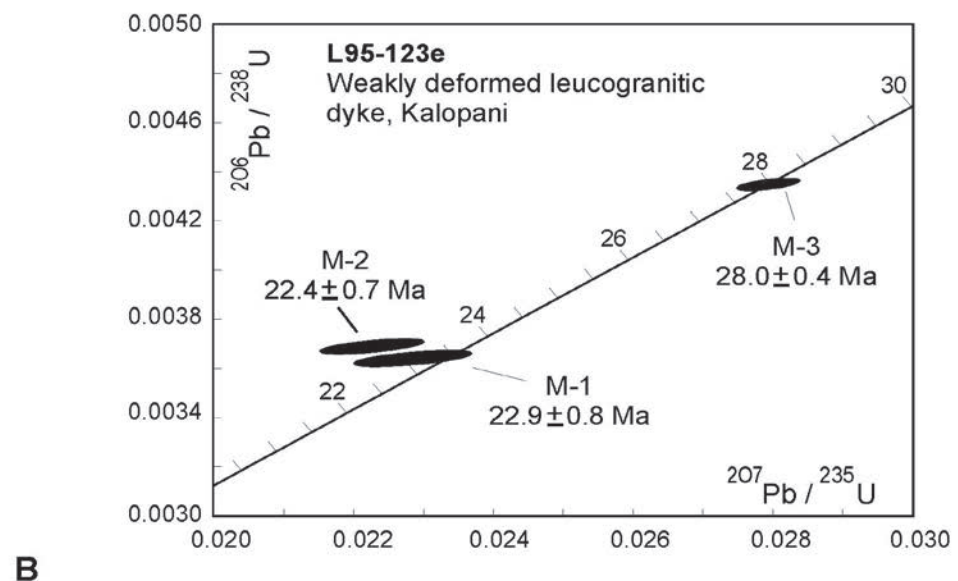
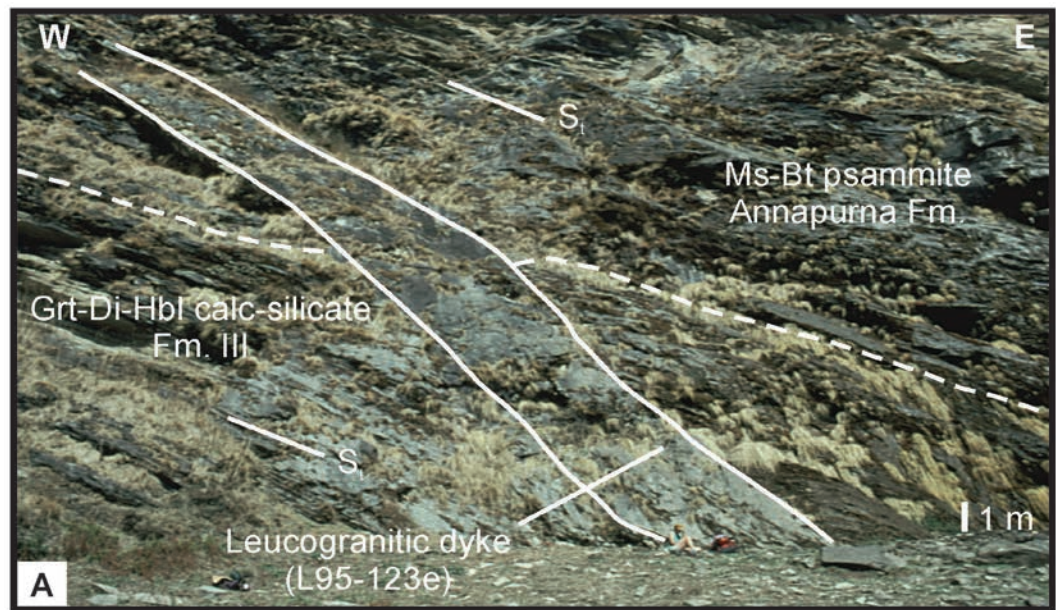
ry between two domains of contrasting structural style. Many workers followed Gansser's observations, and although some speculated or proposed a faulted contact (Bodenhausen and Egeler, 1971; Bordet et al., 1981; Caby et al., 1983; Colchen et al., 1986; Pêcher, 1991), the Annapurna detachment was not clearly documented until the 1990s (Brown and Nazarchuk, 1993).

The Annapurna detachment is characterized by a 1,500-m-thick high strain zone localized in the lowermost part of the Tethyan sedimentary sequence and the uppermost part of the Greater

Himalayan metamorphic sequence (Godin et al., 1999a). The high-strain zone affects the lowermost section of the Ordovician Nilgiri Formation, the entire Annapurna (Yellow-Larjung) Formation (Figs., 16, 17, 18), and the uppermost 100 m of Unit III of the Greater Himalayan metamorphic sequence (Figs, 19, 21).

Several mesoscale shear-sense indicators associated with the high strain zone are readily visible. Shear-sense indicators include systematic asymmetric isoclinal folds and boudins (Figs. 17, 20), extensional shear bands, and S-C fabrics, which

**Figure 18**  
Outcrop photos showing  
a cross-cutting dyke (A)  
and its U-Pb age (B)  
(Godin et al., 2001).



consistently indicate down-to-the northeast normal shearing across the high strain zone (Godin et al., 1999a). Farther to the north-east gray foliated marble of the Ordovician Nilgiri Formation can be observed overlaying the Larjung Formation (Fig. 20d). Other shear-sense indicators include pegmatite dike arrays that have been extended or shortened according to their orientation with respect to the shear plane. Leucogranite dikes (garnet + muscovite + tourmaline) intrude the high-

strain zone (Fig. 18). Similar dykes are not found in the TSS exposed structurally above, nor in the adjacent regions (e. g. Searle and Godin, 2003) apart Jumla-Karnali area in Western Nepal where granites and dykes intrude the TSS (Bertoldi et al., 2011; Carosi et al., 2013a).

According to Godin (2003) several lines of evidence indicate that the high strain zone was affected by subsequent localized southwest-verging deformation. Top-to-the-southwest shear-sense

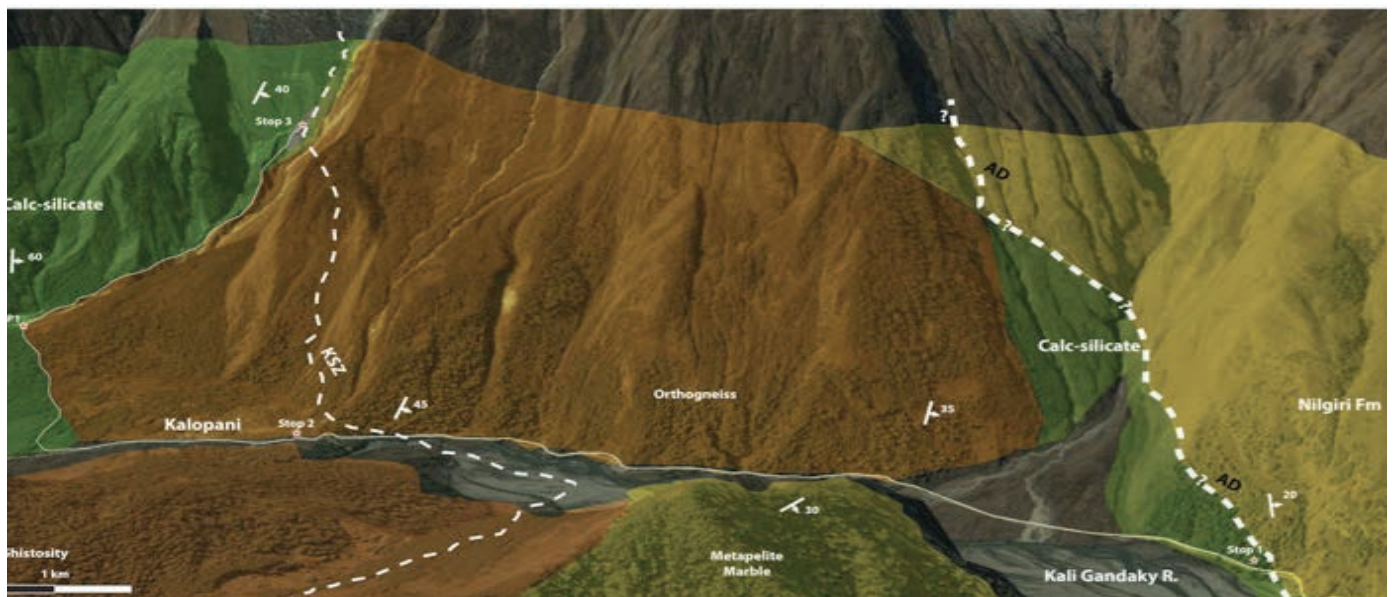


Figure 19

Itinerary of the stops 6-8 and geological feature of the area. The stops are indicated by red stars (Stop1= 6, Stop 2 is 7 and Stop 3 is 8). KSZ: Kalopani shear zone; AD: Annapurna Detachment.

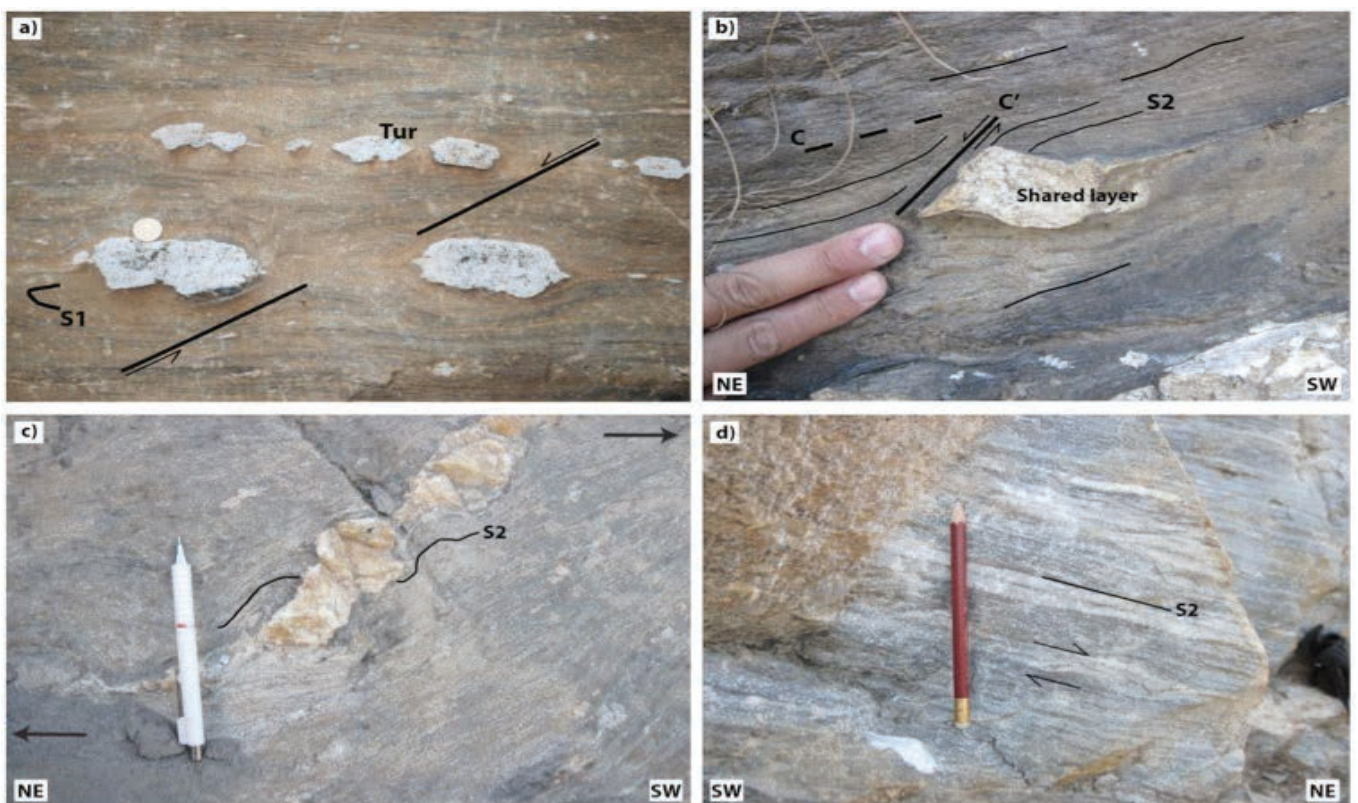
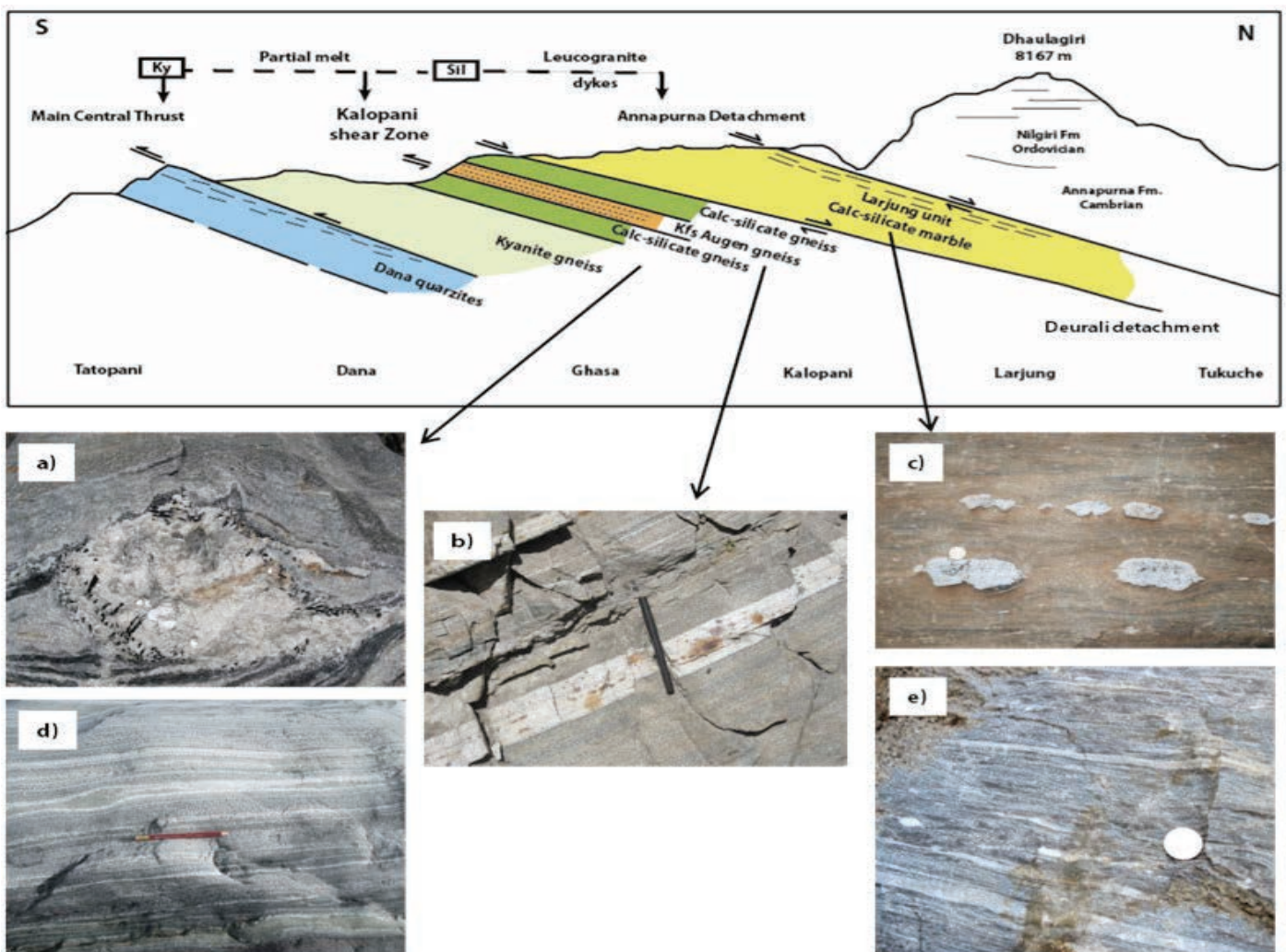


Figure 20

Annapurna Yellow Formation (Larjung Formation). Rocks and associated structures related to the high strain zone of the Annapurna Detachment. A: Shear-type boudins of leucogranitic dykes in the foliated metapelites and calc-silicates. B: Extensional shear band of a leucogranitic dyke affecting the metapelite of the Larjung Formation. C: Flanking fold showing a dextral movement towards the north-east. D: Foliated marble with a rotated centimeter sigma-type quartz-fish pointing a top-to the NE sense of shear.



**Figure 21**

North-south geologic cross section of the Annapurna-Dhaulagiri area in the Kali Gandaki valley. The arrows recall the structural position of the rock types in the images. Modified after Searle (2010). a) muscovite and tourmaline in situ melt from orthogneiss in Unit 3, the leucosome is sheared and shows asymmetric wings; b) sheared tourmaline and garnet leucogranitic dike parallel to the S2 foliation; c) metapelite from Larjung Formation; d) penetrative S2 foliation in a calc-silicate of Unit 2; e) foliated gray marble from Annapurna Yellow Formation (Larjung Formation).

indicators, including oblique boudinaged calcite veins, are locally associated with systematic south-west-verging kinks overprinting the Annapurna detachment fabric (Godin et al., 1999a).

The immediate footwall rocks exposed between Kalopani and Kokhetanti comprise:

- Unit III augen gneiss, which has an interpreted magmatic and crystallization age of  $484 \pm 9$  Ma (Godin et al., 2001). This Ordovician granite is intruding into sillimanite-bearing metapelites that also contain Ordovician monazites, suggesting these rocks preserve a pre-Himalayan Ordovician metamorphic event (Godin et al., 2001).
- Ca. 34 Ma U-Pb monazite and zircon ages

from kyanite-bearing leucosomes interpreted to coincide with Oligocene burial metamorphism of the GHS, coeval with the development of north-verging folds in the overlying TSS (Godin et al., 1999b; 2001).

The immediate hanging-wall rocks (within the high-strain zone) around Kokhetanti:

- Cross-cutting weakly-deformed leucogranitic dikes dated at ca. 22.5 Ma, indicating the ductile strain associated with the Annapurna detachment ceased by ca. 22 Ma (Fig. 18, Godin et al., 2001).

We move to the South toward the village of Kalopani and we enter in the metamorphic sequence of the GHS. The stops 6, 7 and 8 are shown in Fig.

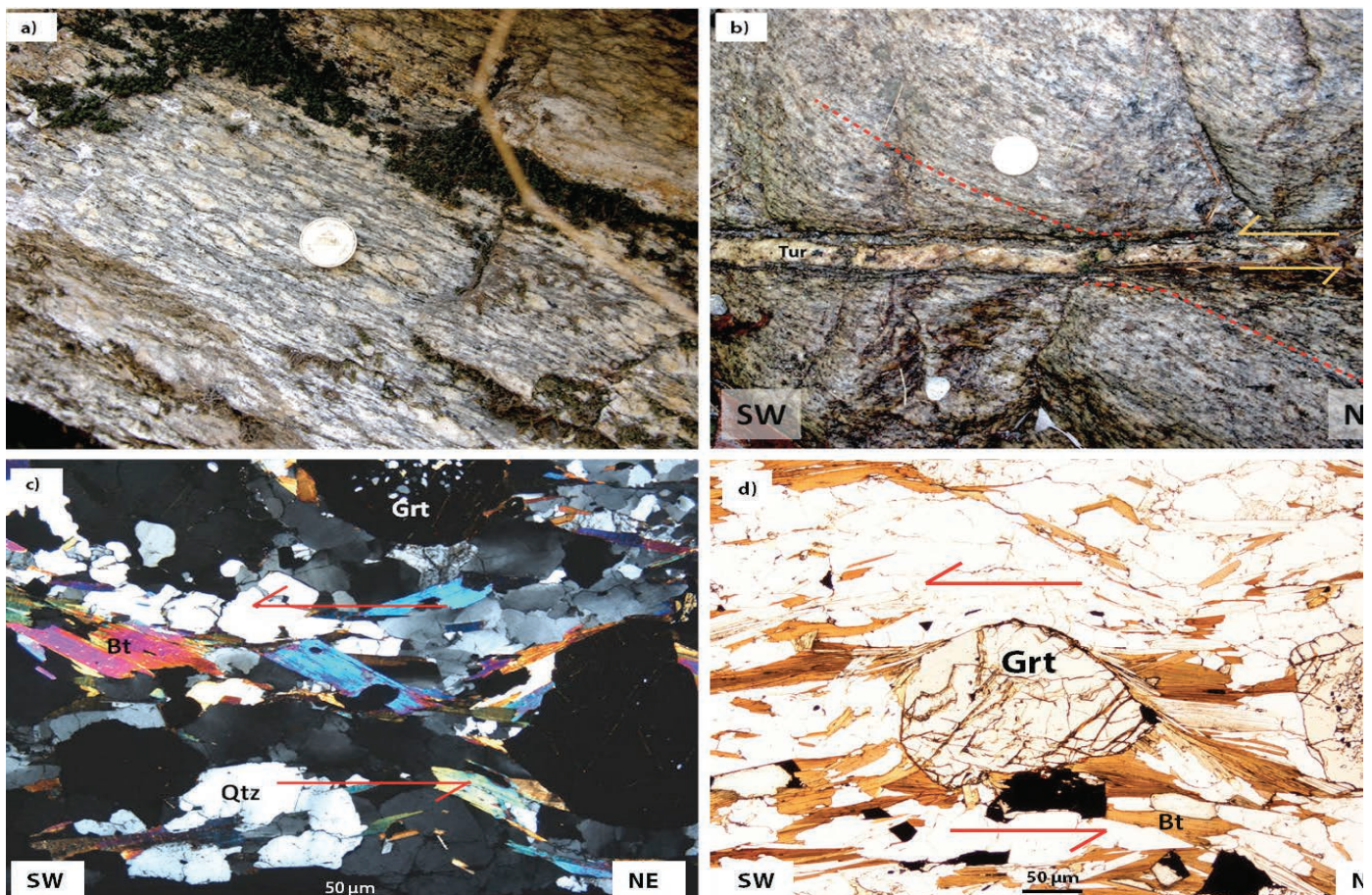


Figure 22

Kalopani shear zone. Outcrop photo (a-b) and microstructure (c-d) of the mylonitic orthogneiss within the high-strain zone with a top-to-the SW sense of shear. A: Outcrop photo of the augen gneiss of unit 3. B: Shear band affected the orthogneiss near Kalopani, the sense of shear is top-to the South-west. The core of the shear band is composed by a Tur leucogranite. The sheared foliation S2 is indicated (red). C: microstructure of the Grt paragneiss (2 nicol), mylonitic fabric and the mica-fish object indicating SW-verging simple shear of the Kalopani shear zone. Lobate contact within quartz ribbon indicating partial recrystallization. Rotated garnet with inclusion trails of quartz (S1 relict). D: Rotated garnet from a KSZ paragneiss (1 nicol).

19 (indicated as 1, 2 and 3 respectively in the figure).

#### Stop 7

Locality: Kalopani-Lete (N28° 38' 37,2" - E83° 35' 43,8")

Theme: Top-to-the South ductile shear zone in the upper part of the GHS.

Near the village of Kalopani, the west side of the valley is characterized by the homoclinal foliation of the GHS dipping moderately to the north (Fig. 21). Proceeding along the main road a few hundreds of meters to the north of Kalopani village we come across a road cut exposing augen gneiss of the Unit 3. The Kalopani shear zone (KSZ; Vannay

and Hodges, 1996) crops out about 1 km north of the village of Kalopani. It is a 20-50 m thick ductile shear zone (Fig. 19) that strikes NW-SE and dips moderately to the NE. Elongated crystals and boudins mark the stretching lineation trending NE-SW and plunging 30-40° to the NE. A mylonitic foliation (S2), which transposes the main foliation, is systematically observed at different scale. S2 is marked by shape-preferred orientation (SPO) of biotite and muscovite (Fig. 21 a-b).

The meso- and micro-scale kinematic indicators such as: shear bands, mineral fish, rotated porphyroclasts, mantled objects and boudins record a top-to the SW sense of shear (Fig. 22 a, b, c). Microstructural observations indicate high-T deformation as evidenced by lobated grain boundaries, quartz/feldspar ribbons, pinning microstructures, blocky undulatory extinction patterns in quartz,

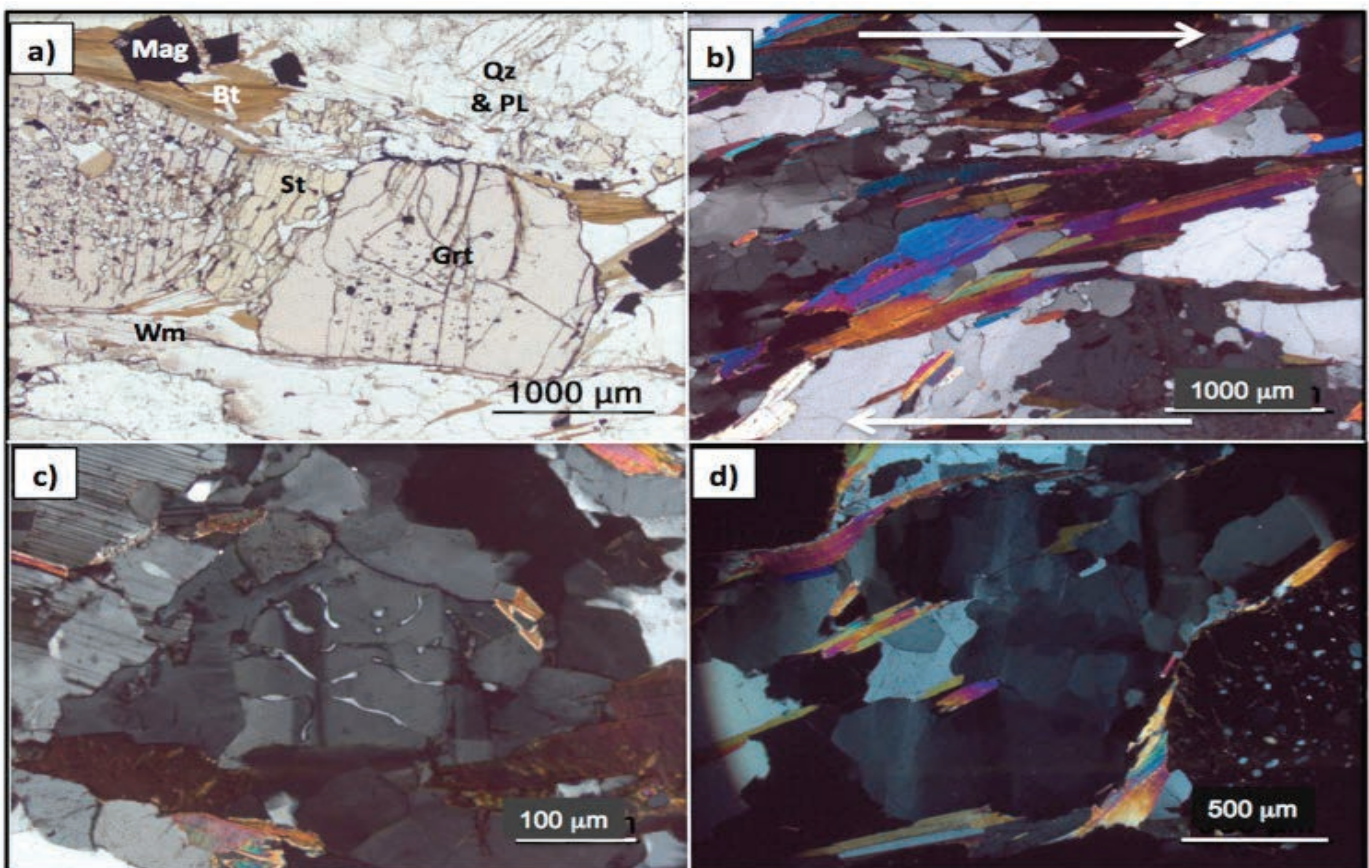


Figure 23

Kalopani shear zone microphotos. a) Garnet and staurolite porphyroclasts in the sheared paragneiss; b) mica fish pointing to a top-to-the South West sense of shear: orthogneiss; c) myrmekitic feldspar in the sheared orthogneiss; d) chess-board extinction in quartz testing simultaneous basal and prismatic slip under high-T conditions: orthogneiss.

and myrmekites (locally asymmetric) in feldspar porphyroclasts (Fig. 23).

Based on  $^{40}\text{Ar}/^{39}\text{Ar}$  geochronology Vannay and Hodges (1996) interpreted movement across the shear zone to be older than 15-13 Ma. Godin et al. (2001) placed further constraints on the shearing to be between 15 Ma and 22.5 Ma. New data in progress obtained by U-Th-Pb in situ isotopic analyses on monazite reveal that shearing could have initiated along the KSZ earlier than 15-22.5 Ma, potentially before 28 Ma (Carosi et al., 2013b).

#### Stop 8

Locality: Lete river valley (N28° 37'40,9" - E83° 34'56,3")

Theme: GHS; contact between Unit 2 and Unit 3.

We move to the south from the village of Kalopani along the main road to Lete village. After walking

nearly 500 m we take a little track in the forest on the west side of the road and we follow it until we find the Lete river (Fig. 19). We follow up the river and at an altitude of nearly 2700 m the river splits in two parts; we follow the northern branch. From this point it is possible to observe mega-scale F2 Nilgiri anticline and refolded F1 fang nappe to the east as explained in the line drawing of Fig. 24.

On the north side (left bank) of the river we cross the orthogneiss of Unit 3, and on the southern side (right bank) green calc-silicate of the Unit 2 is well exposed. The calc-silicate is characterized by a planar penetrative foliation dipping towards the north - north-east.

The contact between the units is parallel to the main foliation that is locally related to large- to small-scale irregular isoclinal folds.

Unit 2 is mainly represented by calc-silicates gneiss and marbles with the mineral assemblage made by  $\text{Qz} + \text{Pl} + \text{Kfs} + \text{Bt} + \text{Ep} + \text{Cpx} + \text{Hbl} + \text{Cal} + \text{Scp} + \text{Grt} + \text{Ms} + \text{Ttn}$  and others acces-

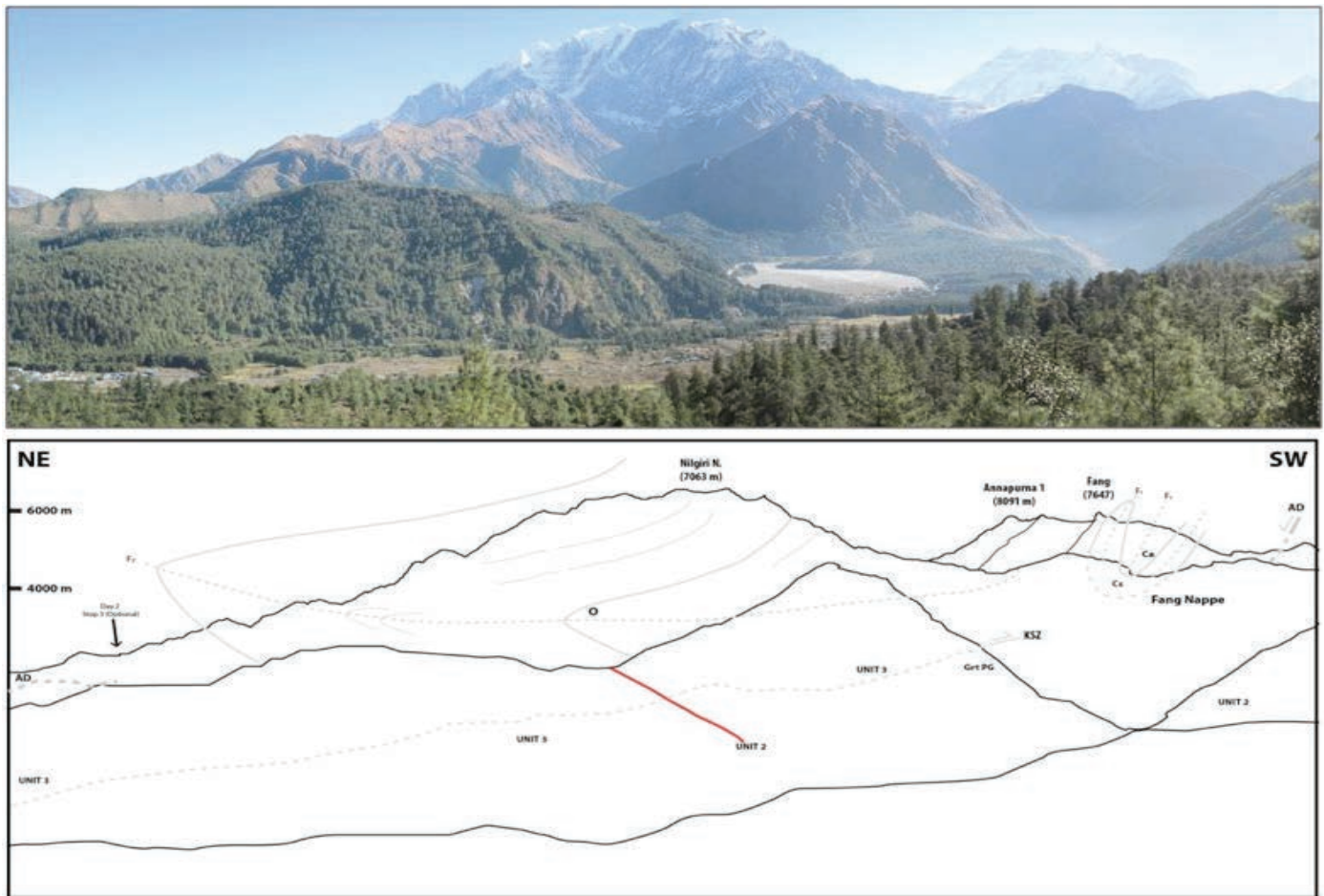


Figure 24

Photograph of the west face of Mt. Nilgiri and Mt. Annapurna as seen from position P1 in fig. GHS-1. The line drawing shows the projected contacts of the Paleozoic units that outline the F2 Nilgiri anticline and the folded F1 Fang nappe. The red line represent the normal fault system associated with the Takkhola graben (Hurtado et al., 2001). AD, Annapurna detachment, KSZ, Kalopani shear zone, CA, Cambrian-Ordovician, CS, Cambrian-Ordovician Sanctuary Formation, O, Ordovician, S, Silurian.

sories (mineral abbreviations after Whitney and Evans, 2010), indicating an upper amphibolite facies metamorphic condition (Miyashiro, 1994; Vannay and Hodges, 1996). Gneiss shows a granoblastic-polygonal texture, suggesting a post-kinematic annealing of the fabric due to GBAR (grain boundary area reduction; Passchier and Trouw, 2005) in amphibolites facies conditions with local fluids redistribution on grain boundary as suggested by coronitic brown amphibole overgrowths on Cpx on cooling. Locally up to 20% (by volume) of leucogranitic bodies (Larson and Godin, 2009) are present (Fig. 25, interpreted as sheared sills and/or transposed dykes. Constraints on metamorphic condition of Unit 2 and on its timing in central Nepal are reported in Kohn and Corrie (2011). These Authors coupled titanite U-Pb geochronology with Zr-in titanite thermometer,

revealing how this calcsilicate rocks have experienced a very high temperature ( $> 700\text{ }^{\circ}\text{C}$  up to  $775\text{ }^{\circ}\text{C}$ ) metamorphism for a long protracted period of time, more than 10 Ma (c. 37 to 24 Ma), before cooling starts around 20 Ma. Similar T values are also recorded by titanites in the calcsilicate of Kali Gandaki transect (Iaccarino S., unpublished data).

Proceeding upward in the valley, close to the river at an altitude of nearly 3000 m (N  $28^{\circ} 37'40,9''$ -E  $83^{\circ} 34'56,3''$ ), we observe a transposed contact between calc-silicate gneiss and a plurimetric tourmaline-garnet leucogranite; interpreted to be units 2 and 3 respectively. In the calc-silicate gneiss the S1 foliation is not exposed at the meso-scale, and F1 axial planes are folded by F2 (Fig. 24 a-b). D2 structures mainly consist of isoclinal folds, from centimeter to metre-size,

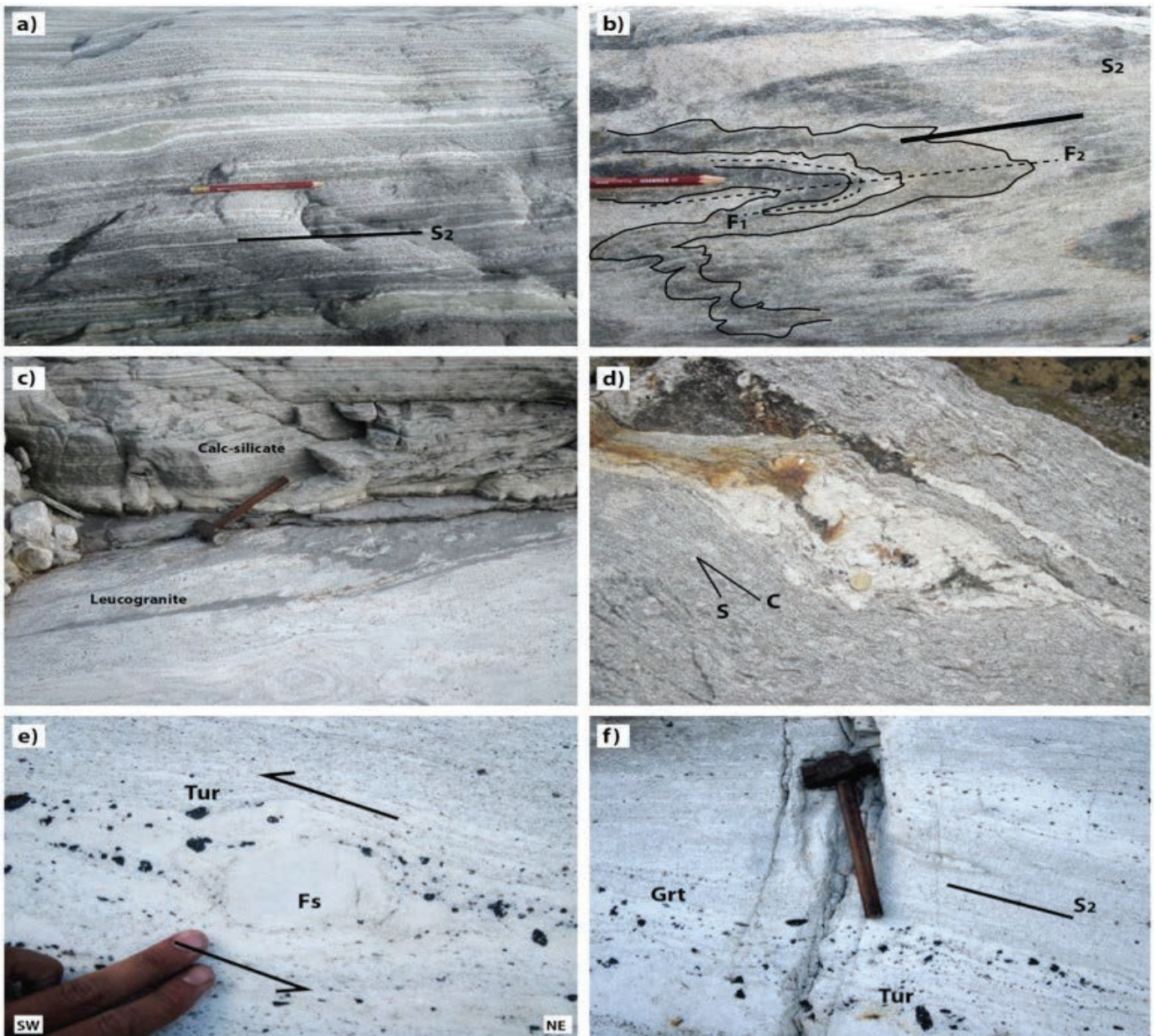


**Figure 25**

Middle GHS rocks from unit 2 and unit 3 exposed in the Lete khola valley. A: Penetrative S2 foliation in the Calc-silicates. B: view of the F1 axial plane folded by the irregular isoclinal folding of F2, and S2 Axial plane foliation in the Calc-silicates. C: Contact between leucogranite and Calc-silicate. D: Tourmaline crystals in situ melt from augen gneiss of unit 3 C-S plain in the mylonitic foliation. E: Centimeter  $\delta$ -type feldspar porphyroclast indicating top-to-the NE sense of shear in the leucogranite. F: Rotated porphyroclasts of tourmaline and garnet in leucogranite.

transposing the S1 foliation into a penetrative S2 axial plane foliation, that varies from spaced to continuous. We observe rotated porphyroclasts of feldspar showing a top-to-the NE sense of shear related to the deformation phase D2. Centimeter to pluri-centimeter crystals of tourmaline and garnet are rotated in deformed leucogranite sills (Fig. 25 e-f).

#### Stop 9

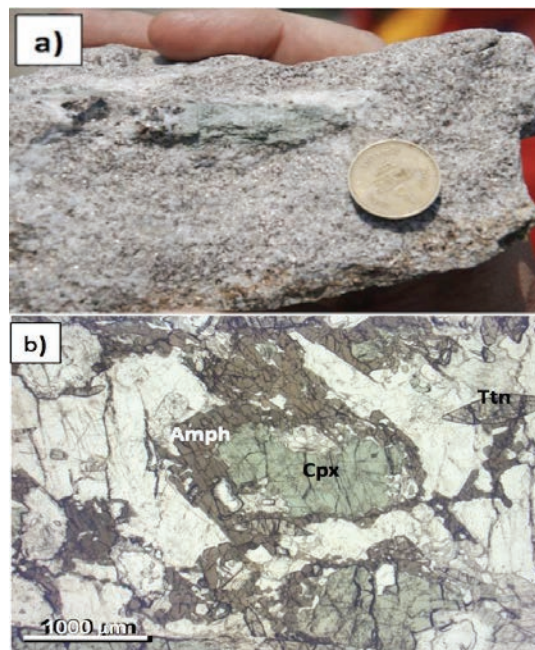
Locality: South of Ghasa village (N 28° 35' 23" E 83° 38' 47")

Theme: GHS; Calc-silicates of Unit 2

Choose a stop near to, but after, the suspension bridge south of Ghasa village to examine the Calc-silicates of Unit 2 and cm-size diopside crys-

Figure 26

Gneiss in Unit 2. a) Cm-size diopside crystal (green) in biotite-gneiss; b) Microphoto showing amphibole coronae on clinopyroxene in a titanite bearing calcisilicate gneiss.



tals (Fig. 26a). In thin section we can observe coronitic amphibole overgrowths on Cpx (Fig. 26b).

#### Stop 10

Locality: N 28° 34' 13"; E 83° 38' 20", 1787 m a.s.l.  
Theme: GHS; biotite- muscovite -kyanite-garnet bearing schist and gneiss of Unit I

This stop roughly corresponds to the stop G42 of the Field Guide book by Upreti and Yoshida (2005).

Following down the road in between Rupse-Chhahara and Titar villages, fresh gneiss and micaschist crop out along the road cut for several kilometers.

The outcrop exposes biotite-muscovite-kyanite-garnet bearing micaschist and gneiss, interlayered dm-thick amphibolite layers containing centimetric garnets (Fig. 27a). The kyanite and garnet in the micaschist and gneiss is cm-size. Kyanite is particularly abundant in quartz veins and quartz-feldspar leucocratic layers parallel to the main foliation along the road cut where this aluminosilicate can reach several cm in size (Fig., 28 b, d).

The mineral assemblage of the gneisses is: Qz + Pl + Bt + Grt + Ky + Ms ± Sil, with locally retrograde Chl. Accessory minerals are Mnz, Ap, Zrn, Tur, Rt, Ilm, Py and rare Xtm.

The main foliation is marked by aligned biotite, white mica, quartz, feldspar and sillimanite and dips moderately to the NE (Figs. 27, 28). It wraps

around garnet and kyanite porphyroclasts. Quartz veins and leucosomes are deformed in tight asymmetric folds, with stretched limbs, verging to the SW (Fig. 27 b, c).

Kinematic indicators include shear bands, C-S fabrics and sigma type-asymmetric tails around garnet porphyroclasts that indicate a top-to-the SW sense of shear (Figs. 27, 28) in agreement to the shearing linked to the MCT few hundreds meters structurally below (Fig. 29a, b).

Needles of fibrolitic sillimanite occur rarely within the fractured kyanite, sometimes at the rims of biotite and muscovite in contact with garnet and at the boundary of plagioclase. This is a microstructural evidence of P-T-path of the rock crossing the stability field of sillimanite after the main assemblage Ky-Bt-Ms-Grt-melt equilibrated (mineral abbreviation according to Whitney and Evans, 2010). The mineral assemblage Qtz + Pl + Bt + Ms ± Grt ± Ky (+ former melt, see below) characterizes the prograde metamorphism (Vanay and Hodges, 1996) whereas the growth of sillimanite occurred later during decompression. A late stage of greenschist facies retrogression is sporadically testified by growth of late Chl on Bt and along cracks of Grt.

It is worth of note that the “peak” P-T estimates of ~ 0.8-1.0 GPa and 600-650°C reported by Vanay and Hodges (1996) on these rocks, based on rim geo-thermobarometry, reflect probably a late re-equilibration as also suggested by recent data based on P-T pseudosection calculation and Zr-in rutile thermometer (Iaccarino, unpublished) as well as the findings of nanotonalites inclusion in garnet (see below).

Both quartz and plagioclase grains show microstructures indicating recovery and dynamic recrystallization processes. Quartz grains have lobate grain boundaries, internal subgrains that are locally formed a chessboard pattern. Plagioclase feldspar also has lobate grain boundaries, deformation twins and a distinct lack of internal microfractures. Kyanite is often twinned and sometimes shows undulose extinction. Pinning and windows microstructures (Passchier and Trouw, 2005) are observed in quartz indicating Grain Boundary Migration recrystallization at relatively high temperature of deformation.

Garnet grains are zoned with a core and inner rim grown during prograde metamorphism whereas the outer rim is interpreted to have grown during retrograde P-T conditions as indicated by compositional X-ray maps (Ca, Mg, Mn and Fe) (Carosi et al., in press).

Figure 27

a) Amphibolite with cm-size garnet bearing layers; b) detail of the foliation with mm-size green amphiboles and deformed garnet and deformed veins with cm-size garnets; c) stretched and isoclinally folded vein along the main foliation; d) biotite and sillimanite bearing mylonitic foliation with asymmetric pressure shadow around garnet with a top-to-the SW sense of shear.

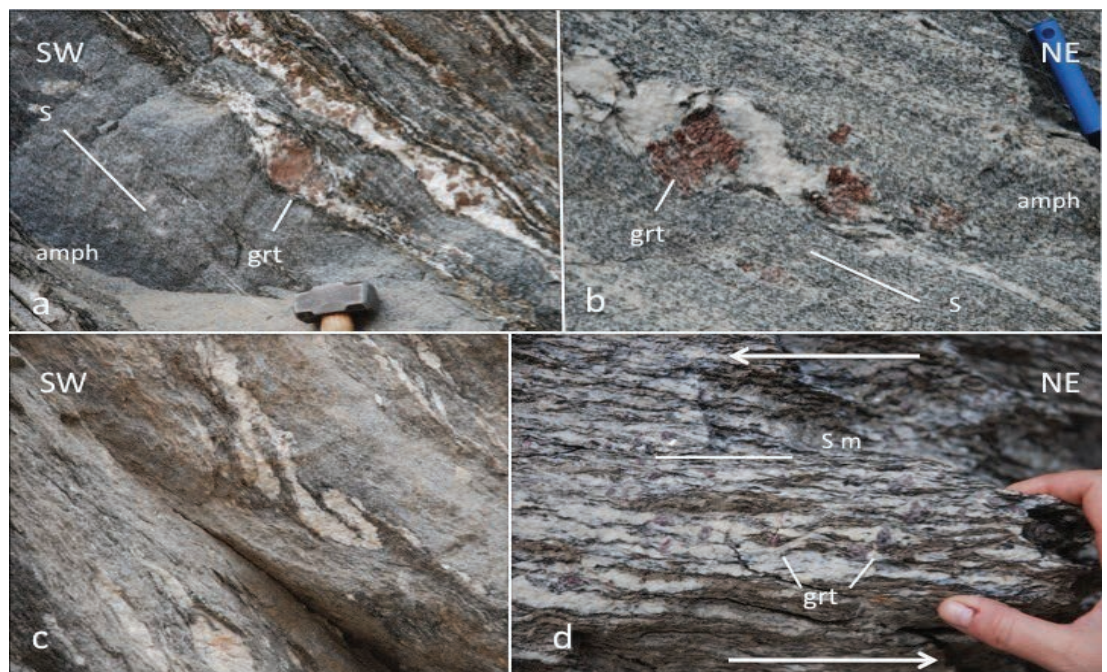
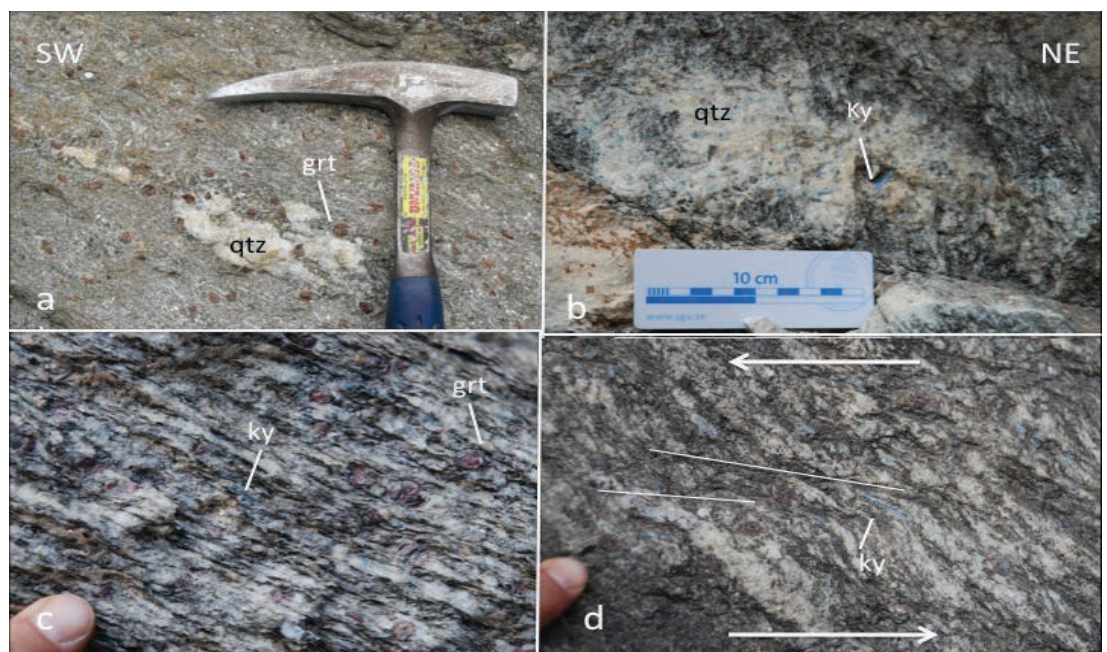


Figure 28

a) Garnet bearing micaschist; b) cm-size kyanite crystals in leucocratic vein; c) kyanite-garnet paragneiss; d) shear bands with a top-to-the SW sense of shear linked to the MCT shearing affecting kyanite and garnet.



It is worth noting that Ca-rich melts (nanotonalites inclusions) have been found in cm-size garnets from this outcrop indicating partial melting in the kyanite stability field (Carosi et al., in press). In situ U-Th-Pb geochronology on monazite in the same microstructural position as the nanotonalites (further confirmed by microchemical zoning in garnet) provide information of the timing of their entrapment at ~ 36-41 Ma during early Eo-Himalayan metamorphism (Carosi et al., in press). Older Eo-Himalayan ages, up to ~ 35

Ma, have been reported also by Godin et al. (2001) in monazite of Unit 3 associated to the generation of kyanite-bearing leucosomes.

The composition of Ca-rich melts is in agreement with the occurrence of similar melts found in the Namche Barwa syntaxis and in southern Tibetan gneiss domes (King et al., 2011; Zeng et al., 2012) produced by muscovite-absent melting under high pressure fluid present conditions. This first stage of melting was followed by the widespread occurrence of younger melts producing

**Figure 29**  
Main Central Thrust near Dana village. Location according to Colchen et al. (1986). a) Phyllites with C-S fabric showing a top-to-the SW sense of shear; b) sigmoidal quartz veins and C-S fabric showing a top-to-the SW sense of shear; c) Quartzite layer dipping to the north just below the kyanite-garnet bearing gneiss and micaschist; d) zoomed-in photo of the foliation surface of the quartzite in c).



**Figure 30**  
C-S fabric in phyllites with abundant deformed quartz veins. Top-to-the SW sense of shear.



the well known high Himalayan Miocene leucogranites during the overall decompression of the GHS. Monazite ages, related to nanogranites in garnets, at 36-41 Ma in Kali Gandaki valley and at 31-28 Ma in Central and Eastern Nepal point to a quite larger time span for the occurrence of melting during prograde metamorphism in the GHS.

#### Stop 11

Locality : Northern end of Dana village (N 28° 31' 27.7" E 83° 39' 31,3")

Theme : Main Central Thrust

Going down after some turns of the road we reach Dana village and nearly 500 m before the village

Figure 31  
Banded quartzite of the  
Fagfog formation.



Figure 32  
Deformation in phyllites  
showing sigmoidal folia-  
tion, C/S/C' fabrics, and  
asymmetric, folded quartz-  
veins. All indicate a top-to-  
the SW sense of shear.



we can observe the sharp contact between kyanite and garnet micaschist and gneiss of the GHS with the quartzites of the LHS. This contact has been considered as the classical MCT (Fig. 29a, b) by Le Fort (1975); Vannay and Hodges (1996); Godin et al. (2001); Godin (2003); Upreti and Yoshida (2005). A medium to dark grey weathering quartzite mylonite with biotite partings crops out a little distance south of this location (Fig 29c, d). It records top to the south sense shear strain and

has an fabric opening angle that is consistent with deformation temperatures of  $\sim 640 \pm 50$  °C (Larson and Godin, 2009). As mentioned previously both the definition and the position of the MCT has been rigorously debated across the Himalayan and other authors, following the definition of Searle et al. (2008), have located the structure farther to the south, near the village of Mahabar (Larson and Godin, 2009; Searle 2010). There, the structure is sometimes referred to as the MCT II

or lower MCT, whereas the MCT near Dana regarded as the MCT I or upper MCT.

#### Stop 12

Locality: Duwari Khola, Duwarikhola village, This stop corresponds to the stop G-47 of the Field Guide book by Upreti and Yoshida (2005); N 28° 31' 41.05", E 083° 39' 04.94"

Theme: Phyllonite (lower part) of the MCT zone

The area between the MCT and the Duwari Khola to the south includes variable phyllonitic and mylonitic, dominantly meta-pelitic rocks of the LHS. Black phyllonitic meta-pelitic rocks are particularly well exposed along the Duwari Khola. The rocks here comprise muscovite, graphite, and biotite and include with light colored disaggregated anatexite(?) pods of quartz + feldspar. The rocks in this exposure have been subjected to top to the south shear deformation. This is recorded as well-developed C/S/C' fabrics (Fig. 30).

#### Stop 13

Locality: Near the bridge on the west bank of the Kali Gandaki River near Gharkholagau; 28° 29' 27.4"N, 083° 38' 57.7"E

Theme: Fagfog Formation and gabbro amphibolite

After passing south, through the village of Tapani (the name of which means 'hot water' as it is located near famous riverside hot springs) quartzite of the Fagfog Formation and intercalated gabbro amphibolite crop out along the road section near to the confluence of Kali Gandaki River and Ghar Khola. Both are characterized by and foliation that dips to the north-northeast. The white to grayish colored quartzite of Fagfog Formation (Fig. 31) consists of coarse-to medium grained recrystallized quartz with fine muscovite partings and thin intercalations of phyllite. A specimen collected from this location yielded a quartz c-axis lattice preferred orientation fabric consistent with deformation at  $\sim 500 \pm 50$  °C (Larson and Godin, 2009). The amphibolite at this locality consists dominantly of medium-to-coarse grained plagioclase, epidote, and hornblende with minor quartz, K-feldspar and biotite. It is interpreted to have a gabbroic protolith.

#### Stop 14

Locality: Confluence of the Beg Khola and Kali Gandaki river; 28° 25' 56.08"N, 083° 35' 59.36"E  
Theme: Kuncha Formation phyllite and the lower MCT (MCT II)

The Kuncha Formation at this location consists of fine-grained gray phyllite with local intercalated metasediment lenses. Disaggregated quartz veins are also common at this locality. The rocks here record evidence of pervasive, high shear strain. C/S/C' fabrics are well developed throughout the outcrop (Fig. 32) and all indicate a top to the south sense of shear. (It is recommended that the outcrop is viewed along the Beg Khola; approximately perpendicular to the tectonic transport direction.) Larson and Godin (2009), using the definition of the Main Central thrust suggested by Searle et al. (2008) that the structure be mapped at the base of Cenozoic metamorphism, cooling, and pervasive ductile deformation, mapped these rocks as part of the Main Central thrust. All rocks structurally higher are pervasively deformed at relatively high temperatures (see quartz deformation temperatures above), while from this location southward the road section towards Beni Bazaar (800 m) is dominated by relatively less strained low-grade phyllitic rocks of the Kuncha Formation.

## REFERENCES

- Aikman, A.B., Harrison, T.M., and Lin, D., 2008. Evidence for early (>44 Ma) Himalayan crustal thickening, Tethyan Himalaya, southeastern Tibet. *Earth and Planetary Science Letters*, 274, 14-23, doi:10.1016/j.epsl.2008.06.038.
- Antolín, B., Appel, A., Montomoli, C., Dunkl, I., Ding, L., Gloaguen, R. and El Bay, R., 2011. Kinematic evolution of the eastern Tethyan Himalaya: constraints from magnetic fabric and structural properties of the Triassic flysch in SE Tibet. In: Poblet, J., Lisle, R. (Eds.), *Kinematic Evolution and Structural Styles of Fold-and-Thrust Belts: Geological Society of London Special Publications*, 349, 99-121.
- Bertoldi, L., Massironi, M., Visonà, D., Carosi, R., Montomoli, C., Gubert, F., Naletto, G., and Pelizzo, M.G., 2011. Mapping the Buraburi granite in the Himalaya of Western Nepal: remote sensing analysis in a collisional belt with vegetation cover and extreme variation of topography. *Remote Sensing of Environment* 115, 1129-1144.

- Bodenhausen, J.W.A. and Egeler, C.G., 1971. On the geology of the upper Kali Gandaki Valley, Nepalese Himalayas. I. Koninkl. Nederl. Akademie van Wetenschappen-Amsterdam, Proceedings, Ser. B 74 (5): 526-538
- Bodenhausen, J.W.A., De Boov, T., Egeler, C.G. and Nijhuis, H.J., 1964. Report on geology of central west Nepal. A preliminary note. In R. K. Sundaran (ed). Himalayan and Alpine orogeny. Proceeding of Section II, XII IGC, New Delhi, 101-122.
- Brown, R.L. and Nazarchuk, J.H., 1993. Annapurna detachment fault in the greater Himalaya of Central Nepal. Geological society of London, 74, 41-473.
- Bordet, P., Colchen, M., Le Fort, P. and Pecher, A., 1981. The geodynamic evolution of the Himalaya. Ten years of research in Central Nepal Himalaya and some other regions. In: Gupta and Delany (Editors), Zagros-Hindu Kush-Himalaya Geodynamic Evolution. Am. Geophys. Union, Geodyn. Ser., 3, 149-168.
- Burg, J.P. and Chen, G.M., 1994. Tectonics and structural zonation of southern Tibet, China. Nature, 311, 219-223.
- Burchfiel, B.C. and Royden, L.H., 1985. North-south extension within the convergent Himalayan region. Geology, 13, 679-682.
- Burchfiel, B. C., Chen, Z., Hodges, K. V., Liu, Y., Royden, L. H., Geng, C. and Xu, J., 1992. The South Tibetan Detachment System Himalayan orogen: extension contemporaneous with and parallel to shortening in a collisional mountain belt. Geol. Soc. America (Sp. Paper), 269, 1-41.
- Caby, R., Pêcher, A. and Le Fort, P., 1983. Le grand chevauchement central himalayen: Nouvelles données sur le métamorphisme inverse à la base de la Dalle du Tibet. Revue de Géologie Dynamique et de Géographie Physique 24, 89-100.
- Carosi, R., Lombardo, B., Musumeci, G. and Pertusati, P.C., 1999. Geology of the Higher Himalayan Crystallines in Khumbu Himal (Eastern Nepal). Journal of Asian Earth Sciences, 17, 785-803.
- Carosi, R., Montomoli, C., and Visonà D., 2002. Is there any detachment in the Lower Dolpo (western Nepal)? Comptes Rendus Geosciences, 334, 933-940,
- Carosi, R., Montomoli, C. and Visonà, D., 2007. A structural transect in the Lower Dolpo: Insights on the tectonic evolution of Western Nepal. Journal of Asian Earth Sciences, 29, 407-423.
- Carosi, R., Montomoli, C., Rubatto, D. and Visonà, D., 2010. Late Oligocene high-temperature shear zones in the core of the Higher Himalayan Crystallines (Lower Dolpo, Western Nepal). Tectonics 29, TC4029. <http://dx.doi.org/10.1029/2008TC002400>.
- Carosi, R., Montomoli, C., Rubatto, D., and Visonà D., 2013a. Leucogranite intruding the South Tibetan Detachment in western Nepal: implications for exhumation models in the Himalayas. Terra Nova, 25, 478-489, doi: 0.1111/ter.12062.
- Carosi, R., Montomoli C., Iaccarino S., Visonà D., 2013b. High Himalayan Discontinuity: a key structure driving the earlier exhumation of the Greater Himalayan Sequence in Central Himalayas. In: 28th Himalayan Karakorum Tibet Workshop and 6th International Symposium on Tibetan Plateau Joint Conference, Tuebingen, Germany, 22-24 August 2013.
- Carosi, R., Montomoli, C., Langone, A., Turina, A., Cesare, B., Iaccarino, S., Fascioli, L., Visonà, D., Ronchi, A. and Rai, S.M., – Eocene partial melting recorded in peritectic garnets from kyanite-gneiss, Greater Himalayan Sequence, central Nepal. In: “Tectonics of Himalayas” (Editors: S. Mukherjee, B. Mukherjee, D. Robinson, R. Carosi), Geol. Soc. London Special Publication, in press
- Colchen, M., Le Fort, P. and Pecher A., 1986. Notice explicative de la carte géologique Annapurna–Manaslu–Ganesh (Himalaya du Népal) au 1:200 000e (bilingual: French–English), CNRS, Paris, 1986.
- Colchen, M., Le Fort, P. and Pêcher, A., 1981. In: Gupta, H.K., Delany, F.M. (Eds.), Geological map of Annapurnas–Manaslu–Ganesh Himalaya of Nepal. Zagros-Hindu Kush-Himalaya geodynamic evolution, Washington, DC (American Geophysical Union, scale 1:200,000).
- Crouzet, C., Dunkl, I., Paudel, L., Arkai, P., Rainer, T.M., Balogh, K. and Appel, E., 2007. Temperature and age constraints on the metamorphism of the Tethyan Himalaya in Central Nepal: a multidisciplinary approach. Journal of Asian Earth Sciences, 30, 113-130
- De Celles, P.G., Gehrels, G.E., Quade, J., Lareau, B. and Spurlin, M., 2000. Tectonic implications of U-Pb zircon ages of the Himalayan orogenic belt in Nepal. Science, 288, 497-499.

- Dunkl, I., Antolín, B., Wemmer, K., Rantitsch, G., Kienast, M., Montomoli, C., Ding, L., Carosi, R., Appel, E., El Bay, R., Xu, Q. and von Eynatten, H., 2011. Metamorphic evolution of the Tethyan Himalayan flysch in SE Tibet. In: Gloaguen, R., Ratschbacher, L. (Eds.), Growth and Collapse of the Tibetan Plateau: Geological Society of London Special Publications, 353, 45–69.
- Fort, M., Freytet, P. and Colchen, M., 1982, Structural and sedimentological evolution of the Thakkhola-Mustang graben (Nepal Himalayas). *Zeitschrift für Geomorphologie*, 42, 75–98.
- Fuchs, G., 1964, Beitrag zur Kenntnis des Paläozoikums und Mesozoikums der Tibetischen Zone in Dolpo (Nepal, Himalaja), *Verh. Geol. Bundesanst.*, 1, 6–15.
- Fuchs, G., 1967. Zum Bau des Himalaya. *österreich. Akad. Wiss., mathem.-naturwiss. Kl., Denkschriften*, 113, Wien, pp. 211.
- Fuchs, G., 1977. The geology of the Karnali and Dolpo regions, western Nepal. *Jahrb. Geol. Bundesanst.*, 120, 165–217.
- Fuchs, G. and Frank, W. 1970. The Geology of West Nepal between the Rivers Kali Gandaki and Thulo Bheri. *Jb. Geol. B.-A., Sdb.* 18, 103 S., Wien.
- Gaetani, M. and Garzanti E., 1991. Multicyclic history of the northern India continental margin (Northwestern Himalaya). *American Association of Petroleum Geologist Bulletin*, 75, 1427-1446.
- Gansser, A., 1964. *Geology of the Himalayas*. New York: Wiley Interscience, 289.
- Garzanti, E., 1999. Stratigraphy and sedimentary history of the Nepal Tethys Himalaya passive margin. *Journal of Asian Earth Sciences*. 17, 805-827.
- Garzanti E., Gorza, M., Martellini, L. & Nicora A., 1994. Transition from diagenesis to metamorphism in the paleozoic to mesozoic succession of the Dolpo-Manang synclinorium and Thakkhola graben (Nepal Tethys Himalaya). *Eclologiae Geologicae Helvetiae*, 87, 613-632.
- Gibling, M.R., Gradstein, F.M., Kristiansen, I.L., Nagy, M. Sarti M., and Wiedmann J., 1994. Early Cretaceous strata of the Nepal Himalayas: conjugate margins and rift volcanism during Gondwanan breakup. *Journal of the Geological Society of London*, 151, 269–290.
- Godin, L., Brown, R.L., Hanmer, S. and Parrish, R., 1999a. Back folds in the core of the Himalayan orogen: An alternative interpretation. *Geology*, 27, 151-154.
- Godin, L., Brown, R.L. and Hanmer, S., 1999b. High strain zone in the hanging wall of the Annapurna detachment, central Nepal Himalaya, in Macfarlane, A., Sorkhabi, R. B., and Quade, J., eds., *Himalaya and Tibet: Mountain roots to mountain tops: Geological Society of America (Special Paper) 328*, 199–210.
- Godin, L., Parish, R.R., Brown, L. and Hodges, K.V., 2001. Crustal thickening leading to exhumation of the Himalayan Metamorphic core of central Nepal: insight from U-Pb geochronology and  $^{40}\text{Ar}/^{39}\text{Ar}$  thermochronology. *Tectonics*, 20, 729-747.
- Godin, L., 2003. Structural evolution of the Tethyan sedimentary sequence in the Annapurna area, central Nepal Himalaya. *Journal of Asian Earth Sciences*, 22, 307–328.
- Godin, L., Yakymchuk C., and Harris, L.B. 2011. Himalayan hinterland-verging superstructure folds related to foreland-directed infrastructure ductile flow: insights from centrifuge analogue modelling. *Journal of Structural Geology*, 33, 329-342
- Gradstein, F.M., von Rad, U., Gibling, M.R., Jansa, L.F., Kaminski, M.A., Kristiansen, I.-L., Ogg, J.G., Rohl, U., Sarti, M., Thorow, J.W., Westermann, G.E.G. and Wiedmann, J., 1992. The Mesozoic continental margin of central Nepal. *Geologisches Jahrbuch*, 77.
- Guillot, S., Pêcher, A., Rochette, P. and Le Fort, P., 1993. The emplacement of the Manaslu granite of Central Nepal: field and magnetic susceptibility constraints. In: Treolar, P.J., Searle, M. (Eds.), *Himalayan Tectonics Geological Society Special Publication*, 74, 413–428.
- Heim, A. and Gansser, A., 1939. Central Himalaya: geological observations of the Swiss expedition 1936. *Memoir Society Helvetica Science Nature* 73, 1–245
- Hodges, K.V., 2000. Tectonics of the Himalaya and southern Tibet from two perspectives. *Geological Society of America Bulletin*, 112, 3, 324–350.
- Hurtado, J.M., Hodges, K.V. and Whipple, K.X., 2001. Neotectonics of the Thakkhola graben and implications for recent activity on the South Tibetan fault system in the central Nepal Himalaya. *Geological Society of America Bulletin*, 113, 2, 222–240.
- Kellett, D.A. and Godin, L. 2009. Pre-Miocene deformation of the Himalayan superstructure,

- Hidden valley, central Nepal. *Journal of the Geological Society*, 166, 261-275
- King, J., Harris, N., Argles, T., Parrish, R. and Zhang, H., 2011. Contribution of crustal anatectis to the tectonic evolution of Indian crust beneath southern Tibet. *Geological Society of America Bulletin*, 123, 218-239.
- Kohn, M.J. and Corrie, S., 2011. Preserved Zr-temperatures and U-Pb ages in high-grade metamorphic titanite: Evidence for a static hot channel in the Himalayan orogen. *Earth and Planetary Science Letters*, 311, 136-143.
- Larson, K.P. and Godin, L., 2009. Kinematics of the Greater Himalayan sequence, Dhaulagiri Himal: implications for the structural framework of central Nepal. *Journal of the Geological Society*, 166, 25-43, 2009.
- Le Fort, P., 1975. Himalaya: the collided range. *American Journal of Science* 275, 1-44.
- Lombardo B., Pertusati P. C. and Borghi S. 1993. Geology and tectonomagmatic evolution of the eastern Himalaya along the Chomolungma-Makalu transect. In *Himalayan Tectonics*, (Edited by Treolar P. J. and Searle M. P.), pp. 341-355, Geological Society of London Special Publication 74.
- Miyashiro, A., 1994. *Metamorphic Petrology*. Oxford University Press, New York.
- Montomoli, C., Carosi, R. and Visonà, D., 2013. The South Tibetan Detachment System: Thermal and mechanical transition from deeper to upper structural levels. *Geophysical Research Abstracts Vol. 15, EGU2013-6589*, 2013, EGU General Assembly Vienna, 2013.
- Myrow, P.M., Hughes, N.C., Searle, M.P., Fanning, C.M., Peng, S.C. and Parcha, S.K., 2009. Stratigraphic correlation of Cambrian-Ordovician deposits along the Himalaya: implications for the age and nature of rocks in the Mount Everest region. *Geological Society of America Bulletin* 121, 323-332.
- Parrish, R.R. and Hodges, K.V., 1996. Isotopic constrains on the age and provenance of the Lesser and Greater Himalayan sequences, Nepalese Himalaya. *Geological Society of America Bulletin*, 108, 904-911.
- Passchier, C.W., Trouw, R.A.J., 2005. *Microtectonics*. Springer, Berlin, p. 366.
- Pêcher, A., 1978. Déformations et métamorphisme associés à une zone de cisaillement. Exemple du grand chevauchement central himalayen (MCT), transversale des Annapurna et du Manaslu, Népal, Ph. D., Grenoble, 310 p.
- Pêcher, A., 1991. The contact between the higher Himalaya crystallines and the Tibetan sedimentary series: Miocene large-scale dextral shearing. *Tectonics*, 10, 587-598 doi: 10.1029/90TC02655
- Pêcher, A., Le Fort, P., 1986. The metamorphism in Central Himalaya, its relations with the thrust tectonic. In: Le Fort, P., Colchen, M., Montenat, C. (Eds.), *Evolution des domaines orogéniques d'Asie méridionale (de la Turquie à l'Indonésie)* Science de la Terre, Nancy, 47 p. 285-309.
- Pognante, U., Castelli, D., Benna, P., Genovese, G., Oberli, F., Meier, M. and Tonarini, S. 1990. The crystalline units of the High Himalayan sequence in the Lahul-Zaskar region (North-west India); metamorphic-tectonic history and geochronology of collided and imbricated Indian Plate. *Geological Magazine*, 127, 101-116.
- Rai, S. M., Upreti, B.N., Yoshida, M., Bhattarai, T.N., Ulak, P.D., Dahal, R.K., Dhakal, S., Gajurel, A.P. and Koirala, M.P., 2005. *Geology of the Lesser and Higher Himalayan zones along the Kaligandaki Valley, central-west Nepal Himalaya*. Proceeding of JICA Regional Seminar on National Disaster, Kathmandu, Nepal, 43-56.
- Robinson, D.M., DeCelles, P.G., Patchett, P.J. and Garzion, C.N., 2001. The kinematic evolution of the Nepalese Himalaya interpreted from Nd isotopes. *Earth and Planetary Science Letters*, 192, 507-521.
- Schelling, D., 1992. The tectonostratigraphy and structure of the eastern Nepal Himalaya. *Tectonics*, 11, 925-943, doi:10.1029/92TC00213
- Searle, M.P. and Godin, L., 2003. The South Tibetan Detachment System and the Manaslu Leucogranite: a structural reinterpretation and restoration of the Annapurna-Manaslu Himalaya, Nepal. *Journal of Geology*, 111, 505-523.
- Searle M.P., Law R.D., Godin L., Larson K.P., Streule M.J., Cottle J.M. and Jessup, M.J., 2008. Defining the Himalayan Main Central Thrust in Nepal. *Journal of Geological Society of London*, 165, 523-534.
- Searle, P.M., 2010. Low-angle normal faults in the compressional Himalayan orogen; Evidence from the Annapurna-Dhaulagiri Himalaya, Nepal. *Lithosphere*, 6, 4, 296-315.
- Upreti, B.N. 1999. An overview of the stratigraphy and tectonics of the Nepal Himalaya. *Journal of Asian Earth Sciences*, 17, 577-606.
- Upreti, B.N. and Yoshida M., 2005. *Guide book*

- for Himalayan trekkers. Series No.1 . Geology and Natural Harzards along the Kaligandaki Valley, Nepal. Department of Geology, Tri-Chandra Campus, Tribhuvan University, Kathmandu, Nepal, 165 pp.
- Vannay, J.-C. and Hodges, K.V., 1996. Tectono-metamorphic evolution of the Himalayan metamorphic core between the Annapurna and Dhaulagiri, central Nepal. *Journal of Metamorphic Geology*, 14, 635-656.
- Visonà, D. and Lombardo, B., 2002. Two-mica and tourmaline leucogranites from Everest-Makalu region (Nepal-Tibet). Himalayan leucogranites genesis by isobathic heating? *Lithos* 62, 125-150.
- Visonà, D., Carosi, R., Montomoli, C., Peruzzo, L. and Tiepolo, M., 2012. Miocene andalusite leucogranite in central-east Himalaya (Everest-Masang Kang area): low-pressure melting during heating. *Lithos*, 144, 194-208.
- Whitney, D.L. and Evans, B.W., 2010. Abbreviations for names of rock-forming minerals. *American Mineralogist*, 95, 185-187.
- Yin, A., 2006. Cenozoic tectonic evolution of the Himalayan orogen as constrained by along-strike variation of structural geometry, exhumation history, and foreland sedimentation. *Earth-Science Reviews*, 76, 1-131.
- Yoshida, M., Rai, S. M. and Upreti, B.N., 2005. Mylonite and ultramylonite along the main Central Thrust in the Kaligandaki area, west-central Nepal Himalaya. Abstract, 20th Himalaya-Karakorum-Tibet workshop, *Geologie Alpine, Memoire H. S. N. 44*, Aussois, France, 198.
- Zeng, L., Gao, Li-E., Dong, C. and Tang, S. 2012. High-pressure melting of metapelite and the formation of Ca-rich granitic melts in the Namche Barwa Massif, southern Tibet. *Gonwana Research*, 21, 138-151.